Eur. Phys. J. C 2, 95–122 (1998)

THE EUROPEAN PHYSICAL JOURNAL C

Analysis of electroweak precision data and prospects for future improvements

Kaoru Hagiwara[1,2], Dieter Haidt[3], Seiji Matsumoto[1]

[1] Theory Group, KEK, Tsukuba, Ibaraki 305, Japan (e-mail: kaoru.hagiwara@kek.jp)
[2] ICEPP, University of Tokyo, Hongo, Bunkyo-ku, Tokyo 113, Japan (e-mail: seiji.matsumoto@kek.jp)
[3] DESY, Notkestrasse 85, D-22603 Hamburg, Germany (e-mail: haidt@dice2.desy.de)

Received: 18 June 1997

Abstract. We update our previous work on an analysis of the electroweak data by including new and partly preliminary data available up to the 1996 summer conferences. The new results on the Z partial decay widths into b and c hadrons now offer a consistent interpretation of all data in the minimal standard model. The value extracted for the strong interaction coupling constant $\alpha_s(m_Z)$ agrees well with determinations in other areas. New constraints on the universal parameters S, T and U are obtained from the updated measurements. No signal of new physics is found in the S, T, U analysis once the SM contributions with $m_t \sim 175$GeV and those of not a too heavy Higgs boson are accounted for. The naive QCD-like technicolor model is now ruled out at the 99% CL even for the minimal model with $\mathrm{SU}(2)_{\mathrm{TC}}$. In the absence of a significant new physics effect in the electroweak observables, constraints on masses of the top quark, m_t, and Higgs boson, m_H, are derived as a function of α_s and the QED effective coupling $\bar{\alpha}(m_Z^2)$. The preferred range of m_H depends rather strongly on the actual value of m_t: $m_H < 360\,\mathrm{GeV}$ for $m_t = 170\,\mathrm{GeV}$, while $m_H > 130\,\mathrm{GeV}$ for $m_t = 180\,\mathrm{GeV}$ at 95% CL. Prospects due to forthcoming improved measurements of asymmetries, the mass of the weak boson W m_W, m_t and $\bar{\alpha}(m_Z^2)$ are discussed. Anticipating uncertainties of 0.00020 for $\bar{s}^2(m_Z^2)$, 20 MeV for m_W, and 2 GeV for m_t, the new physics contributions to the S, T, U parameters will be constrained more severely, and, within the SM, the logarithm of the Higgs mass can be constrained to about ± 0.35. The better constraints on S, T, U and on m_H within the minimal SM should be accompanied with matching precision in $\bar{\alpha}(m_Z^2)$.

1 Introduction

The physics program of LEP1 is completed and has brought a wealth of precise data at the Z-resonance. With the presentation of the updated measurements at the 1996 summer conferences [1] an appropriate moment has come to assess the impact of the new data in the context of the theoretical framework introduced in [2,3].

The Z-shape variables are now quite well measured (see Table 1), also the apparent discrepancy of the previous R_b and R_c measurements [4] with their Standard Model (SM) expectations seems to be solved. After combining the preliminary data from all LEP experiments and from SLD, the R_c value is now in good agreement with the SM, while R_b is less than 2 standard deviations away from the SM prediction. These new measurements are of importance when extracting a reliable value for the QCD coupling constant $\alpha_s(m_Z)$ from the electroweak data.

The paper is organized as follows. In Sect. 2 all electroweak measurements from LEP, SLC and Tevatron reported to the Warsaw Conference [1], are collected. These data are compared with the SM predictions [2] and a few remarkable features are pointed out. In Sect. 3 a brief review is given of the electroweak radiative corrections in generic $\mathrm{SU}(2)_{\mathrm{L}} \times \mathrm{U}(1)_{\mathrm{Y}}$ models following the formalism of [2]. In Sect. 4 the impact of the new measurements is discussed, in particular the Z-shape parameter measurements at LEP/SLC and the new neutrino measurement of CCFR. A comprehensive fit to all the electroweak data is performed in terms of the three parameters [5] S, T, U, which characterize possible new physics contributions through the electroweak gauge-boson propagator corrections, and $\bar{\delta}_b$ which characterizes possible new physics contributions to the Zb_Lb_L vertex. Section 5 is devoted to the interpretation of all electroweak data within the minimal SM. Their constraints are shown as functions of $\alpha_s(m_Z)$ and $\bar{\alpha}(m_Z^2)$ in the (m_t, m_H)-plane. A brief discussion on the significance of bosonic radiative corrections containing the weak boson self-couplings is also given. In Sect. 6 the impact of future improved measurements of the Z boson asymmetries, the W and top-quark masses and $\bar{\alpha}(m_Z^2)$ are studied. Finally, Sect. 7 gives a summary and outlook.

2 Electroweak precision data

Since our first analysis of electroweak data [2] a considerable improvement occurred in three areas, which is sum-

Table 1. Summary of new electroweak results since our first analysis [2]. These data represent the status as of the 1996 summer conferences and contain contributions from LEP and SLC [1] and Tevatron, $p\bar{p}$ [6] and CCFR [7]. The SM predictions [2] are calculated for $m_t = 175$ GeV, $m_H = 100$ GeV, $\alpha_s(m_Z) = 0.118$, and $1/\bar{\alpha}(m_Z^2) = 128.75$; see Sect. 3 for the definition of $\bar{\alpha}(m_Z^2)$ and its uncertainty. Heavy flavor results are obtained by combining data from LEP and SLC [1]

		data	SM	$\frac{\langle\text{data}\rangle - \text{SM}}{(\text{error})}$
LEP	line shape:			
	m_Z(GeV)	91.1863 ± 0.0020	—	—
	Γ_Z(GeV)	2.4946 ± 0.0027	2.4972	−1.0
	σ_h^0(nb)	41.508 ± 0.056	41.474	0.6
	$R_\ell \equiv \Gamma_{h/}\Gamma_\ell$	20.778 ± 0.029	20.747	1.1
	$A_{\rm FB}^{0,\ell}$	0.0174 ± 0.0010	0.0168	0.6
	τ polarization:			
	A_τ	0.1401 ± 0.0067	0.1485	−1.3
	A_e	0.1382 ± 0.0076	0.1486	−1.4
	heavy flavor results:			
	$R_b \equiv \Gamma_{b/}\Gamma_h$	0.2178 ± 0.0011	0.2157	1.9
	$R_c \equiv \Gamma_{c/}\Gamma_h$	0.1715 ± 0.0056	0.1721	−0.1
	$A_{\rm FB}^{0,b}$	0.0979 ± 0.0023	0.1041	−2.7
	$A_{\rm FB}^{0,c}$	0.0735 ± 0.0048	0.0747	−0.2
	jet charge asymmetry:			
	$\sin^2\theta_{\rm eff}^{\rm lept}(\langle Q_{FB}\rangle)$	0.2320 ± 0.0010	0.2313	0.7
SLC	A_{LR}^0	0.1542 ± 0.0037	0.1485	1.5
	A_b	0.863 ± 0.049	0.935	−1.5
	A_c	0.625 ± 0.084	0.668	−0.5
Tevatron $p\bar{p}$	m_W	80.356 ± 0.125	80.400	−0.4
CCFR	K	0.5626 ± 0.0060	0.5669	0.7

marized in Table 1. The LEP Electroweak Working Group [1] has updated their results by including their preliminary electroweak data available up to summer 1996. The table contains also the results from SLC [1] and new Tevatron data on the W mass [6] and the neutrino neutral current experiment [7]. Correlation matrices among the errors of the line-shape parameters and the heavy-quark parameters are given in Tables 2 and 3, respectively. All the numerical results presented in this paper are based on the unchanged data in [2] and the updated data in Tables 1–3, unless otherwise stated. Also shown in Table 1 are the SM predictions [2] for $m_t = 175$ GeV, equal to the present best value from CDF and D0 [8], $m_H = 100$ GeV, $\alpha_s(m_Z) = 0.118$ and $1/\bar{\alpha}(m_Z^2) = 128.75$. The sensitivity of the fit results due to the uncertainties of the QCD and QED running coupling strengths will be discussed in Sects. 4, 5 and 6. The right-most column gives the difference between the mean of the data and the corresponding SM prediction in units of the experimental error. The data and the SM predictions agree fairly well. The previously [4] larger values of R_b and smaller values of R_c are now close to the SM prediction.

Table 2. The error correlation matrix for the Z line-shape parameters [1]

	m_Z	Γ_Z	$\sigma_{\rm h}^0$	R_ℓ	$A_{\rm FB}^{0,\ell}$
m_Z	1.00	0.09	−0.01	−0.01	0.08
Γ_Z	0.09	1.00	−0.14	−0.01	0.00
$\sigma_{\rm h}^0$	−0.01	−0.14	1.00	0.15	0.01
R_ℓ	−0.01	−0.01	0.15	1.00	0.01
$A_{\rm FB}^{0,\ell}$	0.08	0.00	0.01	0.01	1.00

Table 3. The error correlation matrix for the b and c quark results [1]

	R_b	R_c	$A_{\rm FB}^{0,b}$	$A_{\rm FB}^{0,c}$	A_b	A_c
R_b	1.00	−0.23	0.00	0.00	−0.03	0.01
R_c	−0.23	1.00	0.04	−0.06	0.05	−0.07
$A_{\rm FB}^{0,b}$	0.00	0.04	1.00	0.10	0.04	0.02
$A_{\rm FB}^{0,c}$	0.00	−0.06	0.10	1.00	0.01	0.10
A_b	−0.03	0.05	0.04	0.01	1.00	0.12
A_c	0.01	−0.07	0.02	0.10	0.12	1.00

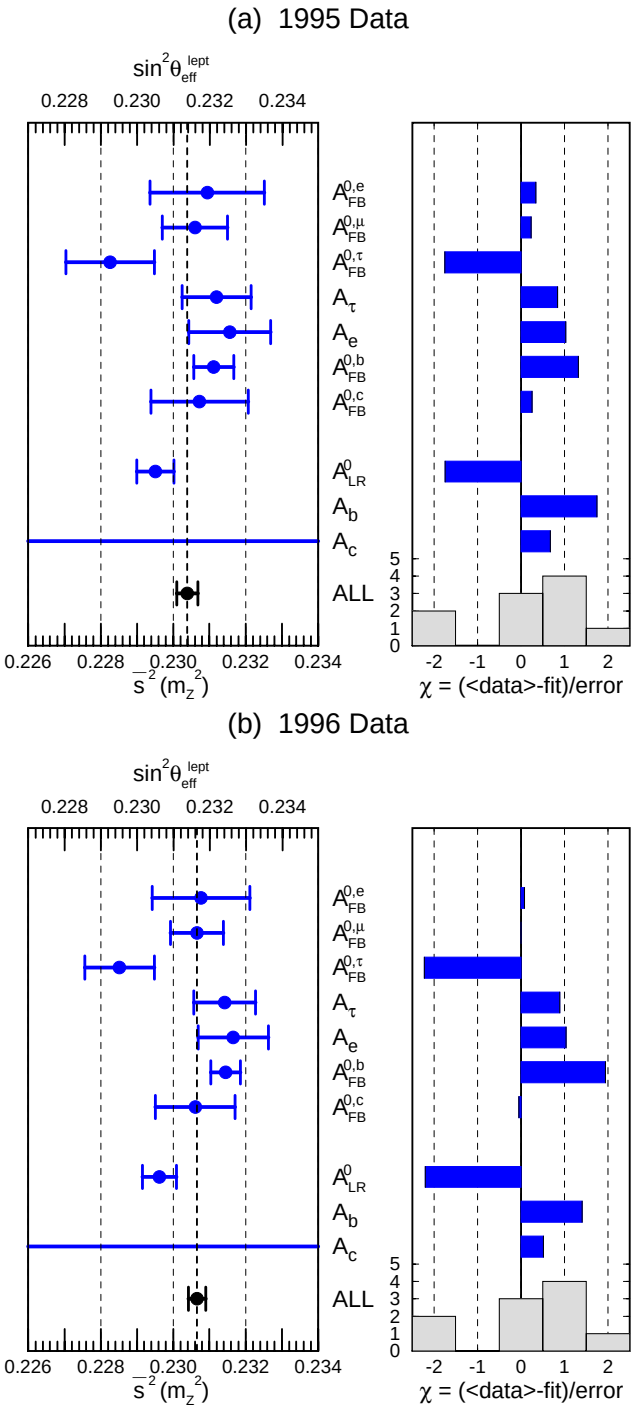

Fig. 1. The effective electroweak mixing parameter $\bar{s}^2(m_Z^2)$ is determined from the asymmetry data from LEP and SLC. The data up to 1995 and up to 1996 are displayed separately. The effective parameter $\sin^2\theta_{\rm eff}^{\rm lept}$ of the LEP Electroweak Working Group[1,4] is related to $\bar{s}^2(m_Z^2)$ [2] by $\sin^2\theta_{\rm eff}^{\rm lept} \approx \bar{s}^2(m_Z^2) + 0.0010$. The A_b-measurement is off scale

All the asymmetry data, including the left-right beam-polarization asymmetry, $A_{\rm LR}$, from SLC are compared in Fig. 1. It shows the result of a one-parameter fit to the asymmetry data in terms of the effective electroweak mixing angle, $\bar{s}^2(m_Z^2)$ [2]. In the SM (for details see Sect. 4) its numerical value is related to the effective parameter $\sin^2\theta_{\rm eff}^{\rm lept}$ adopted by the LEP group [1,4] as follows : $\bar{s}^2(m_Z^2) \approx \sin^2\theta_{\rm eff}^{\rm lept} - 0.0010$ [2]. The lepton forward-backward asymmetry is shown separately for each species. The fit to all 10 measurements yields :

$$\bar{s}^2(m_Z^2) = 0.23065 \pm 0.00024 \qquad (2.1)$$

with $\chi^2_{\rm min}/({\rm d.o.f.}) = 17.3/(9)$. The updated measurements of the asymmetries barely agree (4% CL) with the hypothesis of being determined by a universal electroweak mixing parameter. The new fit is slightly worse than the corresponding one to the 1995 data [4] which gave [9] $\bar{s}^2(m_Z^2) = 0.23039 \pm 0.00029$ with $\chi^2_{\rm min}/({\rm d.o.f.}) = 13.0/(9)$ or 16% CL.

In the analysis presented below we use the data of Table 1 and combine, assuming lepton (e–μ–τ) universality, the three forward-backward lepton asymmetries into the average forward-backward lepton asymmetry $A_{\rm FB}^{\ell,0}$ on the Z-pole. Using the data of Table 1 with $A_{\rm FB}^{\ell,0}$ instead of the three separate asymmetry measurements (see Fig. 1) one obtains :

$$\bar{s}^2(m_Z^2) = 0.23064 \pm 0.00025 \qquad (2.2)$$

with $\chi^2_{\rm min}/({\rm d.o.f}) = 14.1/(7)$. Both the value and the probability of the fit (5% CL) remain nearly unchanged compared to (2.1). The somewhat low probability of the fits reflects the fact that two of the most accurate measurements, $A_{\rm LR}^0$ and $A_{\rm FB}^{b,0}$, are about two standard deviations from the mean to opposite sides as seen in Fig. 1. For instance, ignoring all hadron jet asymmetries and performing the fit with the lepton asymmetry data alone ($A_{\rm FB}^{\ell,0}$, A_τ, A_e $A_{\rm LR}^0$) one obtains

$$\bar{s}^2(m_Z^2) = 0.23019 \pm 0.00031 \qquad (2.3)$$

with $\chi^2/({\rm d.o.f}) = 6.0/(3)$. The fitted mean value decreases by about two standard deviations and the probability of the fit improves to 11% CL.

The quantity K in Table 1 is a new measurement [7] obtained by the CCFR Collaboration from their neutrino data.

The value of the W-mass has been slightly improved [6].

3 Theoretical framework – brief review of electroweak radiative corrections in $\mathbf{SU(2)_L \times U(1)_Y}$ models

The formalism introduced in [2] is used to interpret the electroweak data. We use only those electroweak data that are most model independent, such as those listed in Table 1 of this report and those in Table 6 of [2]. We then

express them in terms of the S-matrix elements of the processes with external quarks and leptons (with or without external QED and QCD corrections, depending on how the electroweak data are evaluated by experiments). These S-matrix elements are then evaluated in a generic SU(2)$\times$U(1) model with four charge form factors, $\bar{e}^2(q^2)$, $\bar{s}^2(q^2)$, $\bar{g}_Z^2(q^2)$ and $\bar{g}_W^2(q^2)$. An additional parameter $\bar{\delta}_b(m_Z^2)$ related to the Zb_Lb_L vertex form factor is also introduced. By assuming negligible new physics contribution to the remaining vertex and box corrections, we derive constraints on the 4+1 form factors from the model-independent data. By further assuming negligible new physics contribution to the running of the charge form factors, we derive constraints on S, T, U and $\bar{\delta}_b(m_Z^2)$. Finally, by assuming no new physics contribution at all, we can constrain m_t and m_H. In this section a brief review of the salient features are given.

The propagator corrections in generic $\mathrm{SU(2)_L \times U(1)_Y}$ models can be conveniently expressed in terms of the following four effective charge form factors [2]:

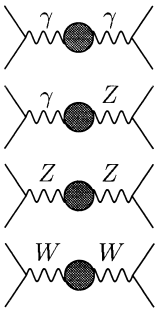

$$\sim \bar{e}^2(q^2) = \hat{e}^2\Big[1 - \mathrm{Re}\overline{\Pi}^{\gamma\gamma}_{T,\gamma}(q^2)\Big], \quad (3.1a)$$

$$\sim \bar{s}^2(q^2) = \hat{s}^2\Big[1 + \frac{\hat{c}}{\hat{s}}\,\mathrm{Re}\,\overline{\Pi}^{\gamma Z}_{T,\gamma}(q^2)\Big], \quad (3.1b)$$

$$\sim \bar{g}_Z^2(q^2) = \hat{g}_Z^2\Big[1 - \mathrm{Re}\overline{\Pi}^{ZZ}_{T,Z}(q^2)\Big], \quad (3.1c)$$

$$\sim \bar{g}_W^2(q^2) = \hat{g}^2\Big[1 - \mathrm{Re}\overline{\Pi}^{WW}_{T,W}(q^2)\Big], \quad (3.1d)$$

where $\overline{\Pi}^{AB}_{T,V}(q^2) \equiv [\overline{\Pi}^{AB}_{T}(q^2) - \overline{\Pi}^{AB}_{T}(m_V^2)]/(q^2 - m_V^2)$ are the propagator correction factors that appear in the S-matrix elements after the weak boson mass renormalization is performed, and $\hat{e} \equiv \hat{g}\hat{s} \equiv \hat{g}_Z\hat{s}\hat{c}$ are the $\overline{\mathrm{MS}}$ couplings. The 'overlines' denote the inclusion of the pinch terms [10,11], which make these effective charges useful [2, 12–14] even at very high energies ($|q^2| \gg m_Z^2$). The amplitudes are then expressed in terms of these charge form factors plus appropriate vertex and box corrections. In our analysis [2] we assumed that all the vertex and box corrections are dominated by the SM contributions, except for the Zb_Lb_L vertex,

$$\Gamma_L^{Zbb}(q^2) = -\hat{g}_Z\Big\{-\frac{1}{2}[1 + \bar{\delta}_b(q^2)] + \frac{1}{3}\hat{s}^2[1 + \Gamma_1^{b_L}(q^2)]\Big\}, \quad (3.2)$$

for which the function $\bar{\delta}_b(m_Z^2)$ is allowed to take on an arbitrary value. Hence the charge form factors and $\bar{\delta}_b$ can be directly extracted from the experimental data and their values be compared with the theoretical predictions.

We *define* [2] the S, T, and U variables of [5] in terms the effective charges,

$$\frac{\bar{s}^2(m_Z^2)\bar{c}^2(m_Z^2)}{\bar{\alpha}(m_Z^2)} - \frac{4\pi}{\bar{g}_Z^2(0)} \equiv \frac{S}{4}, \quad (3.3a)$$

$$\frac{\bar{s}^2(m_Z^2)}{\bar{\alpha}(m_Z^2)} - \frac{4\pi}{\bar{g}_W^2(0)} \equiv \frac{S+U}{4}, \quad (3.3b)$$

$$1 - \frac{\bar{g}_W^2(0)}{m_W^2}\frac{m_Z^2}{\bar{g}_Z^2(0)} \equiv \alpha T, \quad (3.3c)$$

where it is made manifest that these variables measure deviations from the tree-level universality of the electroweak gauge boson couplings. Here $\bar{c}^2 = 1 - \bar{s}^2$ and $\bar{\alpha}(q^2) = \bar{e}^2(q^2)/4\pi$. They receive contributions from both the SM radiative effects and new physics contributions. The S, T, U variables [5] as introduced by Peskin and Takeuchi are obtained [2] approximately by subtracting the SM contributions (at $m_H = 1000$ GeV).

For a given electroweak model we can calculate the S, T, U parameters (T is a free parameter in models without the custodial SU(2) symmetry), and the charge form factors are then fixed by the following identities [2]:

$$\frac{1}{\bar{g}_Z^2(0)} = \frac{1 + \bar{\delta}_G - \alpha T}{4\sqrt{2}\,G_F\,m_Z^2}, \quad (3.4a)$$

$$\bar{s}^2(m_Z^2) = \frac{1}{2} - \sqrt{\frac{1}{4} - \bar{\alpha}(m_Z^2)\Big(\frac{4\pi}{\bar{g}_Z^2(0)} + \frac{S}{4}\Big)}, \quad (3.4b)$$

$$\frac{4\pi}{\bar{g}_W^2(0)} = \frac{\bar{s}^2(m_Z^2)}{\bar{\alpha}^2(m_Z^2)} - \frac{1}{4}(S+U). \quad (3.4c)$$

Here $\bar{\delta}_G$ is the vertex and box correction to the muon lifetime [15] after subtracting the pinch term [2]:

$$G_F = \frac{\bar{g}_W^2(0) + \hat{g}^2\bar{\delta}_G}{4\sqrt{2}m_W^2}. \quad (3.5)$$

In the SM, $\bar{\delta}_G = 0.0055$ [2].

It is clear from the above identities that once we know T and $\bar{\delta}_G$ in a given model we can predict $\bar{g}_Z^2(0)$, and then with the knowledge of S and $\bar{\alpha}(m_Z^2)$ we can calculate $\bar{s}^2(m_Z^2)$, and with the further knowledge of U we can calculate $\bar{g}_W^2(0)$. Since $\bar{\alpha}(0) = \alpha$ is known precisely, all four charge form factors are fixed at one q^2 point. The q^2-dependence of the form factors can also be calculated in a given model, but it is less dependent on physics at very high energies [2]. In the following analysis we assume that the SM contribution governs the running of the charge form factors between $q^2 = 0$ and $q^2 = m_Z^2$. We can then predict all the neutral-current amplitudes in terms of S and T, and the additional knowledge of U gives the W mass via (3.5).

We should note here that our prediction for the effective mixing parameter $\bar{s}^2(m_Z^2)$ is not only sensitive to the S and T parameters but also on the precise value of $\bar{\alpha}(m_Z^2)$. This is the reason why our predictions for the asymmetries measured at LEP/SLC and, consequently, the experimental constraint on S extracted from the asymmetry data are sensitive to $\bar{\alpha}(m_Z^2)$. In order to keep track of the uncertainty associated with $\bar{\alpha}(m_Z^2)$ the parameter δ_α was introduced in [2] as follows: $1/\bar{\alpha}(m_Z^2) \equiv 4\pi/\bar{e}^2(m_Z^2) = 128.72 + \delta_\alpha$. We show in Table 4 the results of the four

most recent updates [16–19] on the hadronic contribution to the running of the effective QED coupling. Three definitions of the running QED coupling are compared. The effective charge $\bar{\alpha}(m_Z^2)$ should be used in (3.3) and (3.4), since the effective charges in (3.1) contain both fermionic and bosonic contributions to the gauge boson propagator corrections.

The new and some earlier estimates [21–23] are also shown in Fig. 2. The analysis of [2] was based on the estimate [23], $\delta_\alpha = 0.00 \pm 0.10$. The last four estimates made use of essentially the same total cross section data set for the process $e^+e^- \to$ hadrons between the two-pion threshold and the Z mass scale. The estimates are slightly different reflecting different procedures adopted by each group to interpolate between the available data points. Eidelman and Jegerlehner [18] and Burkhardt and Pietrzyk [19] made no assumption on the shape (s-dependence) of the cross section, and hence their errors are conservative. Swartz [17] assumed smoothness of s-dependence of the cross section in order to profit from the smaller point-to-point errors within each experiment. Martin and Zeppenfeld [16] also made use of the smaller experimental point-to-point errors by constraining the overall normalization on the basis of the perturbative QCD prediction with $\alpha_s(m_Z) = 0.118 \pm 0.007$ down to $\sqrt{s} = 3$ GeV. The smaller errors of these two estimates are obtained either because of the data point with the smallest normalization error [17] or because of replacing the large normalization uncertainty by the small uncertainty of the perturbative QCD prediction [16] in the region 3 GeV$< \sqrt{s} <$ 7 GeV. The mean values of the two estimates [16,17] are similar as a result of the fact that the measured cross section of the smallest normalization error in the above region agrees roughly with the perturbative QCD prediction. In the following analysis we adopt as a standard the conservative estimate of [18], i.e. $\delta_\alpha = 0.03 \pm 0.09$ and investigate the sensitivity of our results to the deviation $\delta_\alpha - 0.03$. We also show results of the analysis when the estimate [16] $\delta_\alpha = 0.12 \pm 0.06$ is adopted instead.

Once $\bar{\alpha}(m_Z^2)$ is fixed the charge form factors in (3.4) can be calculated from S, T, U. The following approximate formulae [2] are useful:

$$\bar{g}_Z^2(0) \approx 0.5456 \qquad + 0.0040\, T' , \tag{3.6a}$$

$$\bar{s}^2(m_Z^2) \approx 0.2334 + 0.0036\, S' - 0.0024\, T' , \tag{3.6b}$$

$$\bar{g}_W^2(0) \approx 0.4183 - 0.0030\, S' + 0.0044\, T' + 0.0035\, U' , \tag{3.6c}$$

where

$$S' = S - 0.72\, \delta_\alpha , \tag{3.7a}$$

$$T' = T + (0.0055 - \bar{\delta}_G)/\alpha , \tag{3.7b}$$

$$U' = U - 0.22\, \delta_\alpha . \tag{3.7c}$$

The values of $\bar{g}_Z^2(m_Z^2)$ and $\bar{s}^2(0)$ are then calculated from $\bar{g}_Z^2(0)$ and $\bar{s}^2(m_Z^2)$ above, respectively, by assuming the SM running of the form factors. The Z widths are sensitive to $\bar{g}_Z^2(m_Z^2)$, which can be obtained from $\bar{g}_Z^2(0)$ in the SM approximately by

$$\frac{4\pi}{\bar{g}_Z^2(m_Z^2)} \approx \frac{4\pi}{\bar{g}_Z^2(0)} - 0.299 + 0.031 \log\left[1 + \left(\frac{26\text{GeV}}{m_H}\right)^2\right]. \tag{3.8}$$

The approximation is valid to 0.001 provided $m_t > 160\,\text{GeV}$ and $m_H > 40\,\text{GeV}$. On the other hand the low energy neutral current experiments are sensitive to $\bar{s}^2(0)$ which is obtained by assuming the SM running of the charge form factor $\bar{s}^2(q^2)/\bar{\alpha}(q^2)$:

$$\frac{\bar{s}^2(0)}{\alpha} \approx \frac{\bar{s}^2(m_Z^2)}{\bar{\alpha}(m_Z^2)} + 3.09 - \frac{\delta_\alpha}{2}. \tag{3.9}$$

Finally, within the SM the S, T, U parameters and the form factor $\bar{\delta}_b = \bar{\delta}_b(m_Z^2)$ are functions of m_t and m_H which can be parametrized as

$$S_{\rm SM} \approx -0.233 - 0.007 x_t + 0.091 x_H - 0.010 x_H^2 , \tag{3.10a}$$

$$T_{\rm SM} \approx +0.879 + (0.130 - 0.003 x_H) x_t + 0.003 {x_t}^2 - 0.079 x_H - 0.028 x_H^2 + 0.0026 x_H^3 , \tag{3.10b}$$

$$U_{\rm SM} \approx +0.362 + 0.022 x_t - 0.002 x_H , \tag{3.10c}$$

$$\bar{\delta}_{b\rm SM} \approx -0.00995 - 0.00087 x_t - 0.00002 {x_t}^2 , \tag{3.10d}$$

where $x_t = (m_t(\,\text{GeV}) - 175)/10$ and $x_H = \log(m_H(\,\text{GeV})/100)$. The above approximate expressions are valid to ± 0.003 for $S_{\rm SM}$, $T_{\rm SM}$ and $U_{\rm SM}$, and to ± 0.00007 for $\bar{\delta}_{b\rm SM}$ in the domain 160 GeV $< m_t <$ 185 GeV and 40 GeV $< m_H <$ 1000 GeV. They are evaluated after all the two-loop corrections included in [2] are taken into account, for $\alpha_s(m_Z) = 0.118$ in the two-loop $\mathcal{O}(\alpha_s)$ terms [20]. The m_H-dependence of the $\bar{\delta}_b(m_Z^2)_{\rm SM}$ function is found to be negligibly small for the above region of m_t.

Note : Since the publication of our original paper [2] several improvements have been achieved on the SM radiative corrections. Most notably, we now have the three-loop (order α_s^2) QCD calculation of the T parameter [24] as well as in the gauge boson propagator corrections [25]. These three-loop effects slightly modify the relationship between the electroweak S, T, U parameters and the physical top quark mass m_t in the above formulae (3.10). After the completion of the present report we took note of the new evaluation of non-factorizable QCD and electroweak corrections to the hadronic Z boson decay rates [26]. A negative correction to the Z hadronic width was found reducing the SM prediction for Γ_h by 0.59 MeV after summing over the four light quark flavors. The corresponding effect for the partial width $\Gamma(Z \to `b\bar{b}')$ has not been evaluated. This shift would in turn enhance the $\alpha_s$ value extracted from the electroweak data by 0.001. We refrain from modifying the numbers in the present report. If we assume that the corrections to the partial width $\Gamma(Z \to `b\bar{b}')$ is small, the net effect for the numbers due to the above new calculations would be as follows :

Table 4. The running QED coupling at the m_Z scale in the three schemes. $1/\alpha(m_Z^2)_{\rm l.f.}$ contains only the light fermion contributions to the running of the QED coupling constant between $q^2 = 0$ and $q^2 = m_Z^2$. $1/\alpha(m_Z^2)_{\rm f}$ contains all fermion contributions including the top-quark. The values $m_t = 175$ GeV and $\alpha_s(m_Z) = 0.12$ in the perturbative two-loop correction [20] are assumed. $1/\bar{\alpha}(m_Z^2)$ contains also the W-boson-loop contribution [2] including the pinch term [10,11]

	$1/\alpha(m_Z^2)_{\rm l.f.}$	$1/\alpha(m_Z^2)_{\rm f}$	$1/\bar{\alpha}(m_Z^2)$	δ_α
Martin-Zeppenfeld '94 [16]	128.98 ± 0.06	128.99 ± 0.06	128.84 ± 0.06	0.12 ± 0.06
Swartz '95 [17]	128.96 ± 0.06	128.97 ± 0.06	128.82 ± 0.06	0.10 ± 0.06
Eidelman-Jegerlehner '95 [18]	128.89 ± 0.09	128.90 ± 0.09	128.75 ± 0.09	0.03 ± 0.09
Burkhardt-Pietrzyk '95 [19]	128.89 ± 0.10	128.90 ± 0.10	128.76 ± 0.10	0.04 ± 0.10

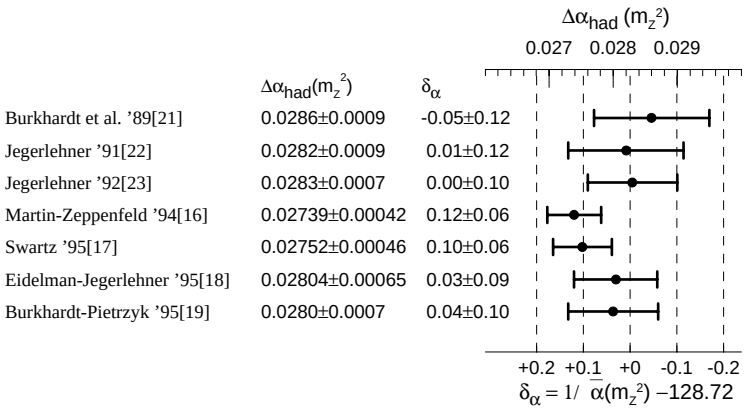

Fig. 2. Various estimates of $\Delta\alpha_{\rm had}(m_Z^2)$ and the resulting $\bar{\alpha}(m_Z^2)$ in the minimal SM. The parameter δ_α [2] is defined as $\delta_\alpha \equiv 1/\bar{\alpha}(m_Z^2) - 128.72$

– The three-loop corrections to the T parameter [24] modifies the relationship (3.10b) between T and the physical top quark mass. By comparing [24] with [2], we find

$$\Big[m_t^{(2-\rm loop)}\Big]^2\Big\{1-\frac{2(3+\pi^2)}{9}\frac{\alpha_s(m_Z)}{\pi}\Big\} = \Big[m_t^{(3-\rm loop)}\Big]^2\Big\{1-\frac{2(3+\pi^2)}{9}\frac{\alpha_s(m_t)}{\pi} -14.594\Big(\frac{\alpha_s(m_t)}{\pi}\Big)^2\Big\}. \quad (3.11)$$

This can be approximated as

$$m_t^{(2-\rm loop)} = m_t^{(3-\rm loop)}\Big\{1-(7.3-5.5\log\frac{m_t}{m_Z}) \times\Big(\frac{\alpha_s(m_Z)}{\pi}\Big)^2\Big\}. \quad (3.12)$$

For $m_t \sim 170\,\text{GeV}$, this corresponds to the replacement of $m_t^{(2-\rm loop)}$ by $m_t^{(3-\rm loop)} - 1\,\text{GeV}$. Non-leading three-loop corrections calculated in [25] modifies $S_{\rm SM}$, $U_{\rm SM}$ in (3.10) and the running of the $\bar{g}_Z^2(q^2)$ charge (3.8). Their effects are, however, much smaller than the leading effect as quoted above. Consequently, the three-loop $\mathcal{O}(\alpha_s^2)$ effects can be approximately taken into account by replacing all the m_t symbols in this report by the r.h.s. combination of (3.12), or roughly by $m_t - 1\,\text{GeV}$. In other words, the fitted m_t value should be about 1 GeV larger, while the results with an external m_t constraint should correspond to those where the external m_t is increased by about 1 GeV.

– The mixed QCD electroweak two-loop corrections of [26] can be accounted for by replacing all α_s symbols in this report by $\alpha_s - 0.001$. In other words, the fitted α_s value should be about 0.001 larger, while the results with an external α_s constraint should correspond to those where the external α_s is increased by about 0.001. This is because the α_s dependences in the corrections other than the hadronic width of the Z are all negligibly small.

4 Implications of the new measurements

In this section the new results and their implications are discussed. Also a fit in terms of the S, T, U parameters [5] of the electroweak gauge boson propagator corrections as well as of the Zb_Lb_L vertex form factor, $\bar{\delta}_b(m_Z^2)$ is presented. The strengths of the QCD and QED couplings at the m_Z scale, $\alpha_s(m_Z)$ and $\bar{\alpha}(m_Z^2)$, are treated as external parameters in the fits, so that implications of their precise knowledge affecting the fit results are made explicit.

4.1 New LEP/SLC data

The updated Z shape parameter measurements (see Tables 1–3) are used to extract the charge form factors. It is assumed that the vertex corrections except for the Zb_Lb_L vertex function $\bar{\delta}_b(m_Z^2)$ are dominated by the SM contri-

butions.[1] The free parameters are : $\bar{g}_Z^2(m_Z^2)$, $\bar{s}^2(m_Z^2)$, α_s' and $\bar{\delta}_b(m_Z^2)$. The quantity α_s' is the combination[2]

$$\alpha_s' = \alpha_s(m_Z)_{\overline{\rm MS}} + 1.54\,[\bar{\delta}_b(m_Z^2) + 0.00995] \qquad (4.1)$$

that appears [2,3] in the theoretical prediction for Γ_h. The fit yields:

$$\left.\begin{aligned} \bar{g}_Z^2(m_Z^2) &= 0.55557 \pm 0.00074 \\ \bar{s}^2(m_Z^2) &= 0.23065 \pm 0.00025 \\ \alpha_s' &= 0.1218 \pm 0.0038 \\ \bar{\delta}_b(m_Z^2) &= -0.0051 \pm 0.0028 \end{aligned}\right\}$$

$$\rho_{\rm corr} = \begin{pmatrix} 1.00 & 0.13 & -0.57 & 0.00 \\ & 1.00 & 0.11 & 0.05 \\ & & 1.00 & 0.01 \\ & & & 1.00 \end{pmatrix}, \qquad (4.2a)$$

$$\chi^2_{\rm min}/({\rm d.o.f.}) = 15.4/(9)\,. \qquad (4.2b)$$

The value of $\chi^2_{\rm min}$ is dominated by the contribution of the asymmetries which accounts for 14.1 (cf. (2.2)). When allowing only $\bar{s}^2(m_Z^2)$ and $\bar{g}_Z^2(m_Z^2)$ to be fitted freely, and treating α_s' and $\bar{\delta}_b(m_Z^2)$ as external parameters, we obtain an equivalent result:

$$\left.\begin{aligned} \bar{g}_Z^2(m_Z^2) &= 0.55557 - 0.00042\,\tfrac{\alpha_s'-0.1218}{0.0038} \pm 0.00061 \\ \bar{s}^2(m_Z^2) &= 0.23065 + 0.00003\,\tfrac{\alpha_s'-0.1218}{0.0038} \pm 0.00024 \end{aligned}\right\}$$

$$\rho_{\rm corr} = 0.24, \qquad (4.3a)$$

$$\chi^2_{\rm min} = 15.4 + \left(\frac{\alpha_s' - 0.1218}{0.0038}\right)^2 + \left(\frac{\bar{\delta}_b + 0.0051}{0.0028}\right)^2. \qquad (4.3b)$$

Compared to the previous results in [2] the precision has increased by more than a factor of two.

The fit can be qualitatively understood as follows. The asymmetries determine almost exclusively $\bar{s}^2(m_Z^2)$. The tiny difference between the above $\bar{s}^2(m_Z^2)$ and (2.2) is due to the α_s'-dependence of R_ℓ. The only quantity constraining $\bar{g}_Z^2(m_Z^2)$ is Γ_Z which also depends on $\bar{s}^2(m_Z^2)$ and α_s', thus explaining the non-negligible error correlations above. The quantity α_s' is mainly determined by R_ℓ and also by σ_h^0. The observable R_b, i.e. the ratio of Γ_b and Γ_h, is constraining $\bar{\delta}_b(m_Z^2)$. It is interesting to note that the form factor $\bar{\delta}_b(m_Z^2)$ is nearly uncorrelated from the other fit quantities because of our using the combination (4.1). It is now straightforward to obtain the best value of α_s from α_s' and $\bar{\delta}_b$:

$$\alpha_s = \alpha_s' - 1.54\,[\bar{\delta}_b + 0.00995\,] = 0.1143 \pm 0.0057\,. \qquad (4.4)$$

[1] We exclude from the fit the jet-charge asymmetry data in Table 1, since it allows an interpretation only within the minimal SM. It is included in our SM fit in Sect. 5

[2] As will be explained in detail in Subsect. 4.2, we modify the definition of α_s' in [2,3] by subtracting the SM contribution to $\bar{\delta}_b(m_Z^2)$ at $m_t = 175\,{\rm GeV}$, $\bar{\delta}_b(m_Z^2) = -0.00995$. See (3.10d)

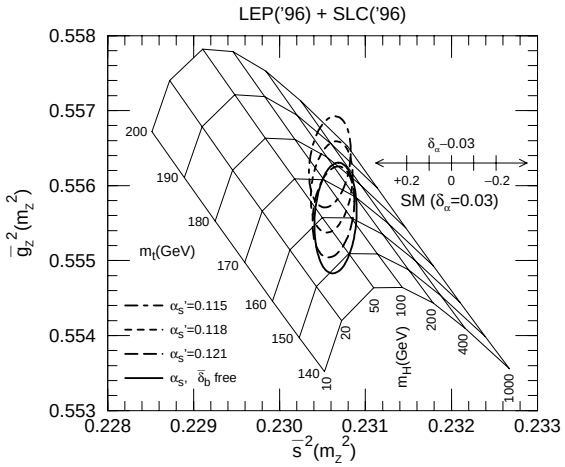

Fig. 3. The 1-sigma allowed contours in $(\bar{s}^2(m_Z^2), \bar{g}_Z^2(m_Z^2))$ plane obtained from the fits to the Z boson parameters. The *solid contour* is obtained by treating α_s' and $\bar{\delta}_b$ as free parameters in the fit. Also shown are the results by treating α_s' as an external parameter. Three values of α_s' (= 0.115, 0.118, 0.121), are chosen. The results are insensitive to the assumed $\bar{\delta}_b$ value. The *grid* illustrates the SM predictions in the range $140\,{\rm GeV} < m_t < 200\,{\rm GeV}$ and $10\,{\rm GeV} < m_H < 1000\,{\rm GeV}$ at $\delta_\alpha \equiv 1/\bar{\alpha}(m_Z^2) - 128.72 = 0.03$, where their dependences on $\delta_\alpha - 0.03$ are shown by a "$\longleftrightarrow$" symbol

If on the other hand R_b and R_c are fixed to their SM predictions with $m_t = 175$ GeV, i.e. $\bar{\delta}_b = -0.00995$, one obtains $\alpha_s = 0.1218 \pm 0.0038$. This little exercise demonstrates the crucial role of the R_b and R_c measurements in obtaining information on α_s from the precision Z experiments.

Figure 3 shows the fit result in the $(\bar{s}^2(m_Z^2), \bar{g}_Z^2(m_Z^2))$ plane. The contours represent the 1-σ (39% CL) allowed region. The solid contour shows the result of the four-parameter fit (4.2). Also shown are the results of the two-parameter fit in terms of $\bar{g}_Z^2(m_Z^2)$ and $\bar{s}^2(m_Z^2)$ treating α_s' as an external parameter. Three values of α_s' (0.115,0.118, 0.121) are chosen in the figure, which correspond respectively to the α_s values in the SM at $m_t = 175\,{\rm GeV}$; see (4.10d). The results are insensitive to the assumed $\bar{\delta}_b$ value once the magnitude of the combination α_s' is fixed. The SM predictions for $\delta_\alpha = 0.03$ and their dependence on $\delta_\alpha - 0.03$ are also given. As expected from (3.6), (3.7) and (3.10), only the predictions for $\bar{s}^2(m_Z^2)$ is sensitive to δ_α.

4.2 The heavy quark sector and α_s

The most striking results of the updated electroweak data are those of R_b and R_c, which are shown in Fig. 4 juxtaposing the status as of summer 1995 and 1996. The SM predictions to these ratios are shown by the thick solid line, where the value of the top-quark mass affecting the Zb_Lb_L vertex correction is indicated by solid blobs. Although it was tempting to conclude from the 1995 data on R_b and R_c that the SM is excluded at 99.99% CL, it was also clear [9,27] that it would be precocious to base

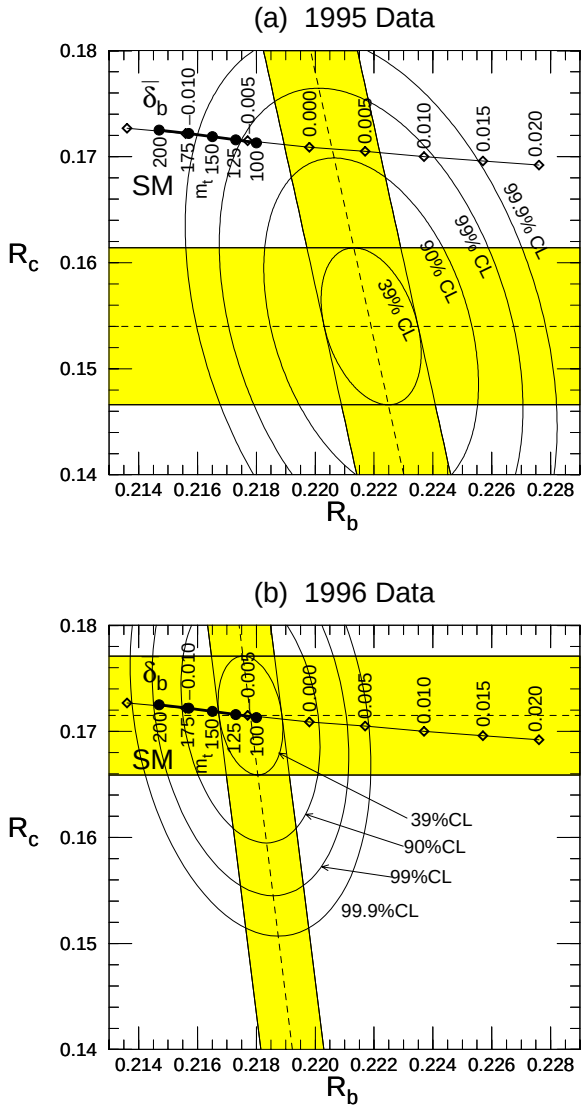

Fig. 4. R_b and R_c data [1,4] and the SM predictions [2]

such a far reaching conclusion on just these two measurements knowing how complex the analyses are and how critical the role of systematic effects is.

It is useful to note the fact that the three most accurately measured line-shape parameters, Γ_Z, σ_h^0 and R_ℓ in Table 1, determine accurately the Z partial widths Γ_l, Γ_h and $\Gamma_{\rm inv}$, because they are three independent combinations of the three partial widths, i.e. $\Gamma_Z = \Gamma_h + 3\Gamma_l + \Gamma_{\rm inv}$, $R_l = \Gamma_h/\Gamma_l$, and $\sigma_h^0 = (12\pi/m_Z^2)\Gamma_h\Gamma_l/\Gamma_Z^2$. We find

$$\begin{aligned}
\Delta\Gamma_h/(\Gamma_h)_{\rm SM} &= 0.0011 \pm 0.0014 \\
\Delta\Gamma_l/(\Gamma_l)_{\rm SM} &= -0.0013 \pm 0.0013 \\
\Delta\Gamma_{\rm inv}/(\Gamma_{\rm inv})_{\rm SM} &= -0.0050 \pm 0.0040 \\
\rho_{\rm corr} &= \begin{pmatrix} 1.00 & 0.49 & -0.41 \\ & 1.00 & 0.23 \\ & & 1.00 \end{pmatrix}, \qquad (4.5)
\end{aligned}$$

where $(\Gamma_h)_{\rm SM} = 1743.4\,{\rm MeV}$, $(\Gamma_\ell)_{\rm SM} = 84.03\,{\rm MeV}$ and $(\Gamma_{\rm inv})_{\rm SM} = 501.9\,{\rm MeV}$ are the SM predictions [2] for $m_t = 175\,{\rm GeV}$, $m_H = 100\,{\rm GeV}$, $\alpha_s = 0.118$ and $\delta_\alpha = 0.03$. The high precision of 0.14% of the hadronic Z partial width, Γ_h, strongly restricts any attempt to modify theoretical predictions for the ratios R_b and R_c [9]. To see this, Γ_h is approximately expressed as

$$\begin{aligned}
\Gamma_h &= \Gamma_u + \Gamma_d + \Gamma_s + \Gamma_c + \Gamma_b + \Gamma_{\rm others} \\
&\sim \{\Gamma_u^0 + \Gamma_d^0 + \Gamma_s^0 + \Gamma_c^0 + \Gamma_b^0\} \\
&\quad \times [1 + \frac{\alpha_s}{\pi} + \mathcal{O}(\frac{\alpha_s}{\pi})^2], \qquad (4.6)
\end{aligned}$$

where Γ_q^0's are the partial widths in the absence of the final state QCD corrections. Hence, to a good approximation, the ratios R_q can be expressed as ratios of Γ_q^0 and their sum. A decrease in R_b and an increase in R_c should then imply a decrease and an increase of Γ_b^0 and Γ_c^0, respectively, from their SM predicted values. The strong interaction coupling α_s acts like a flavor independent adjustment parameter. This is clearly borne out in Fig. 5, where, once *both* Γ_b^0 *and* Γ_c^0 are left free in the fit, the above Γ_h drives α_s for the 1995 data [4] to an unacceptably large value, while for the 1996 update [1] a consistent picture emerges. On the other hand, if we allow only Γ_b^0 to vary by assuming the SM value of Γ_c^0 (the straight line of the extended SM in Fig. 4), then the Γ_h constraint gives a slightly smaller value of α_s, see (4.4), though still compatible with the global average [28], $\alpha_s = 0.118 \pm 0.003$.

In general, if we introduce a fractional change in the bare hadronic width

$$\frac{\delta\Gamma_h^0}{(\Gamma_h^0)_{\rm SM}} \approx \frac{\sum_q \delta\Gamma_q^0}{\sum_q (\Gamma_q^0)_{\rm SM}}\,, \qquad (4.7)$$

one measures to a good approximation from the Z-line shape parameters the combination

$$\alpha_s + \pi \frac{\delta\Gamma_h^0}{(\Gamma_h^0)_{\rm SM}}\,. \qquad (4.8)$$

In other words, the effective parameter α_s'

$$\alpha_s' \equiv \alpha_s(m_Z)_{\overline{\rm MS}} + 3.186 \frac{\delta\Gamma_h^0}{(\Gamma_h^0)_{\rm SM}}\,. \qquad (4.9)$$

is constrained by the Z parameters. The coefficient in front of the fractional width ratio is slightly larger than π because of the higher-order QCD corrections. For definiteness, we use the SM prediction $(\Gamma_h^0)_{\rm SM} = 1678.7\,{\rm MeV}$ evaluated at $(m_t, m_H) = (175, 100)\,{\rm GeV}$. If only the Zb_Lb_L vertex is allowed to deviate from the SM prediction,

$$\begin{aligned}
\alpha_s' &= \alpha_s + 3.186 \frac{\delta R_b}{1 - R_b} && (4.10a) \\
&\approx \alpha_s + 1.54\Big(\bar\delta_b - [(\bar\delta_b)_{\rm SM}]_{m_t = 175\,{\rm GeV}}\Big) && (4.10b) \\
&\approx \alpha_s + 1.54(\bar\delta_b + 0.00995) && (4.10c) \\
&\approx \alpha_s + 0.00134 x_t + 1.54\,[\bar\delta_b]_{\rm NewPhysics} && (4.10d)
\end{aligned}$$

in agreement with the expression (4.1). The last equality is obtained by inserting the SM expression (3.10d) for $\bar\delta_b$

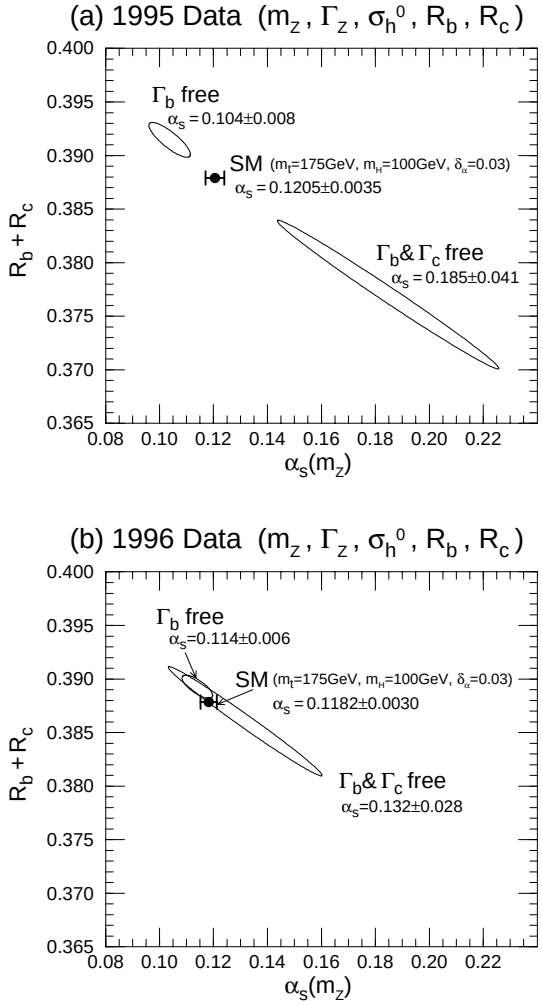

Fig. 5. $R_b + R_c$ vs α_s. From the 1995 data [4] **a** and the 1996 date [1] **b**

where we neglect the small quadratic term. If both R_b and R_c are modified, it is the combination

$$\alpha_s' = \alpha_s + 3.186\frac{\delta R_b + \delta R_c}{1 - R_b - R_c} \tag{4.11}$$

which is constrained by the Γ_h data.

At present, the LEP Collaborations have not yet completed their analyses of R_b and R_c by including the latest runs. However, there are new precise analyses of OPAL on R_c [29] and R_b [30] and one by ALEPH on R_b [31]. The new analyses aim at reducing as much as possible the use of information not directly obtainable from experiment itself. The increased number of tags in the ALEPH analysis implies also a smaller correlation between R_b and R_c. The preliminary values quoted at the 1996 summer conferences [1] roughly agree with the SM expectation and it may now be meaningful to compare the constraints on the strong coupling constant α_s from the Z-pole data with those from other sectors [28] (see Fig. 6). We find the following parametrization for the m_t, m_H and δ_α dependences of the SM fit to α_s:

$$\alpha_s = 0.1182 \pm 0.0030 - 0.00075x_t + 0.0023x_H + 0.00046x_H^2 - 0.00074x_\alpha \tag{4.12}$$

where $x_t = (m_t(\,\mathrm{GeV}) - 175)/10$, $x_H = \log(m_H(\,\mathrm{GeV})/100)$, and $x_\alpha = (\delta_\alpha - 0.03)/0.09$. The parametrization is valid in the range $150 < m_t(\,\mathrm{GeV}) < 200$, $60 < m_H(\,\mathrm{GeV}) < 1000$ and $|\delta_\alpha| < 0.2$. It is remarkable that the electroweak data alone imply an intrinsic precision of ± 0.003 (disregarding new physics contribution to the Z partial widths) which is deteriorated by the imprecise knowledge of the external parameters, i.e. the masses of the top and Higgs and also by the running "QED" coupling $\alpha(m_Z^2)$ (see also Sect. 5.1). It can be seen from Fig. 6 and the above parametrization that the agreement between the SM fit to the Z parameters and the present world average of direct measurements, $\alpha_s = 0.118 \pm 0.003$, is good only for a relatively light Higgs boson ($m_H \lesssim 300\,\mathrm{GeV}$).

4.3 New neutrino data

A new piece of information in the low-energy neutral current sector comes from the CCFR collaboration [7] which measured the neutral- to charged-current cross section ratio in ν_μ scattering off nuclei. Using the model-independent parameters of [32], they constrain the following linear combination,

$$K = 1.732g_L^2 + 1.119g_R^2 - 0.100\delta_L^2 - 0.086\delta_R^2\,, \tag{4.13}$$

and obtain

$$K = 0.5626 \pm 0.0025\,(\mathrm{stat}) \pm 0.0036\,(\mathrm{sys}) \pm 0.0028\,(\mathrm{model}) - 0.0029\,\frac{m_c - 1.31\,\mathrm{GeV}}{0.24\,\mathrm{GeV}}, \tag{4.14}$$

with $m_c = (1.31 \pm 0.24)\,\mathrm{GeV}$. Because of the larger $\langle Q^2\rangle_{\mathrm{CCFR}} = 36\,\mathrm{GeV}^2$ in the CCFR experiments compared to the old data [32] ($\langle Q^2\rangle_{\mathrm{HF}} = 20\,\mathrm{GeV}^2$), the measurement is first expressed in terms of $\bar{s}^2(0)$ and $\bar{g}_Z^2(0)$ and then combined with the old data. Figure 7 shows the CCFR-band together with the ellipse of all previous νq-data.

The CCFR data (4.14) being obtained after correcting for the external photonic corrections lead to the constraint:

$$\bar{s}^2(0) = 0.2421 + 1.987[\bar{g}_Z^2(0) - 0.5486] \pm 0.0058. \tag{4.15}$$

It should be noted that the old data [32] were also corrected for external photonic corrections.[3] We find

$$\left.\begin{aligned} \bar{g}_Z^2(0) &= 0.5454^{+0.0076}_{-0.0082} \\ \bar{s}^2(0) &= 0.2419^{+0.0130}_{-0.0142} \end{aligned}\right\} \quad \rho_{\mathrm{corr}} = 0.916, \tag{4.16a}$$

$$\chi^2_{\mathrm{min}} = 0.13\,. \tag{4.16b}$$

[3] The $\delta_{c.c.}$ correction in [2] was hence erroneously counted twice. The fit (4.17) of [2] has therefore been revised here

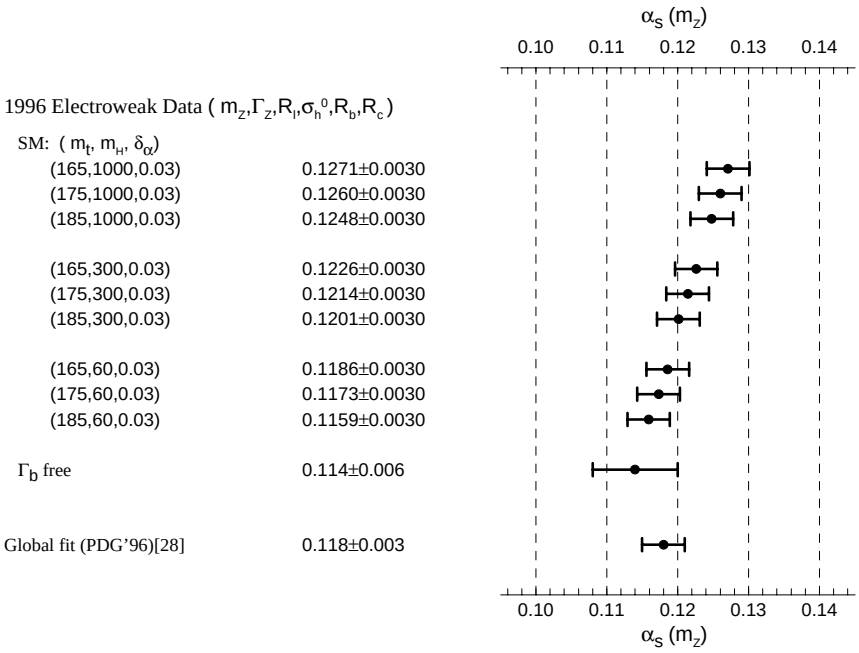

Fig. 6. Constraint on α_s from the electroweak Z boson data by assuming the SM for various m_t and m_H at $\delta_\alpha = 0.03$. Also shown is the result of a more general fit, where Γ_b is a free parameter. For comparison, the global average as obtained by the Particle Data Group [28] is shown

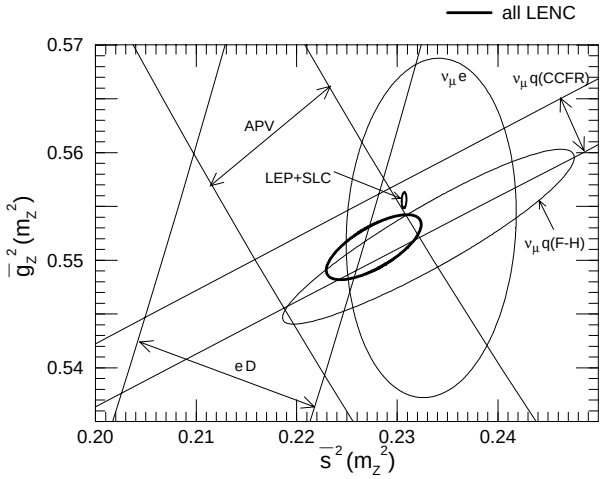

Fig. 7. Fit to the low-energy neutral-current data in terms of the two universal charge form factors $\bar{s}^2(m_Z^2)$ and $\bar{g}_Z^2(m_Z^2)$ which are calculated from $\bar{s}^2(0)$ and $\bar{g}_Z^2(0)$ by assuming the SM running of the charge form factors. 1-σ (39% CL) contours are shown separately for the old [32] and the new [7] ν_μ–q data, the ν_μ–e data, the atomic parity violation (APV) data, and the SLAC e–D polarization asymmetry data: see [2] The 1-σ contour of the combined fit, (4.19), is shown by the *thick ellipse*. The *little ellipse* represents the 1-sigma constraint from LEP/SLC data corresponding to the *solid ellipse* of Fig. 3

The combination of the new CCFR data [7] with the previous neutrino data [32] yields:

$$\left.\begin{aligned}\bar{g}_Z^2(0) &= 0.5476^{+0.0070}_{-0.0076}\\ \bar{s}^2(0) &= 0.2429^{+0.0128}_{-0.0140}\end{aligned}\right\} \quad \rho_{\rm corr} = 0.955, \quad (4.17a)$$

$$\chi^2_{\rm min} = 0.7 \quad ({\rm d.o.f.} = 3). \quad (4.17b)$$

The combined fit to all the low-energy neutral current data including those studied in [2] gives :

$$\left.\begin{aligned}\bar{g}_Z^2(0) &= 0.5441 \pm 0.0029\\ \bar{s}^2(0) &= 0.2362 \pm 0.0044\end{aligned}\right\} \quad \rho_{\rm corr} = 0.70, \quad (4.18a)$$

$$\chi^2_{\rm min} = 2.7 \quad ({\rm d.o.f.} = 8)\,. \quad (4.18b)$$

For later convenience these results are also expressed at the shifted scale $q^2 = m_Z^2$. Here we assume no significant new physics contributions to the running of the charge form factors from 0 to m_Z^2. Uncertainty from the m_H-dependence of the running of $\bar{g}_Z^2(m_Z^2)$, (3.8), is negligibly small for $m_H > 70\,{\rm GeV}$. The result is then :

$$\left.\begin{aligned}\bar{g}_Z^2(m_Z^2) &= 0.5512 \pm 0.0030\\ \bar{s}^2(m_Z^2) &= 0.2277 \pm 0.0047\end{aligned}\right\} \quad \rho_{\rm corr} = 0.70, \quad (4.19a)$$

$$\chi^2_{\rm min} = 2.7 \quad ({\rm d.o.f.} = 8)\,. \quad (4.19b)$$

Figure 7 shows the individual contributions to the fit. The data agree well with each other. Also shown is the combined LEP/SLC fit (the solid ellipse of Fig. 3). Although the low energy data are far less precise than those from the Z resonance, they nevertheless constrain possible new interactions beyond the $\mathrm{SU(2)_L \times U(1)_Y}$ gauge interactions, such as those from an additional Z boson [33].

We may now combine the constraints from the Z parameters, (4.2) and (4.3), and those from the low energy neutral current experiments, (4.19):

$$\left.\begin{aligned}\bar{g}_Z^2(m_Z^2) &= \ 0.55525 \pm 0.00070\\ \bar{s}^2(m_Z^2) &= \ 0.23065 \pm 0.00024\\ \alpha_s' &= \ \ 0.1227 \pm \ \ 0.0037\\ \bar{\delta}_b(m_Z^2) &= -0.0051 \pm \ \ 0.0028\end{aligned}\right\}$$

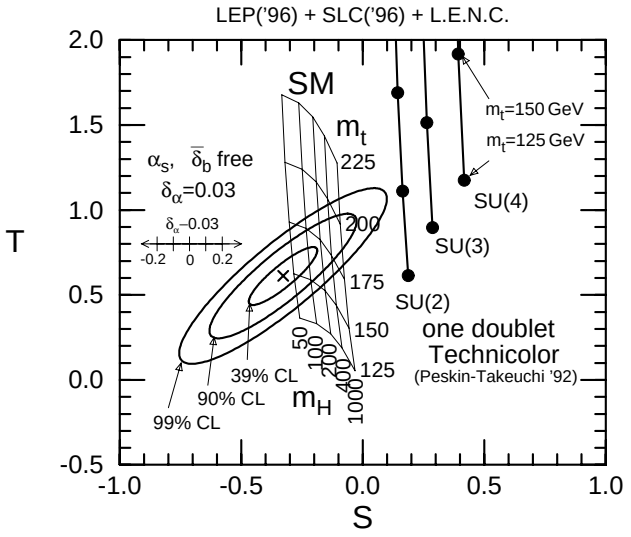

Fig. 8. Constraints on (S, T) from the five-parameter fit to all the electroweak data for $\delta_\alpha = 0.03$ and $\bar{\delta}_G = 0.0055$. Together with S and T, the U parameter, the Zb_Lb_L vertex form factor, $\bar{\delta}_b(m_Z^2)$, and the QCD coupling, $\alpha_s(m_Z)$, are allowed to vary in the fit. Also shown are the SM predictions in the range $125\,\mathrm{GeV} < m_t < 225\,\mathrm{GeV}$ and $50\,\mathrm{GeV} < m_H < 1000\,\mathrm{GeV}$. The predictions [5] of one-doublet SU(N_c)–TC models are shown for $N_c = 2, 3, 4$

$$\rho_{\rm corr} = \begin{pmatrix} 1.00 & 0.14 & -0.54 & 0.00 \\ & 1.00 & 0.11 & 0.05 \\ & & 1.00 & 0.01 \\ & & & 1.00 \end{pmatrix}, \tag{4.20a}$$

$$\chi^2_{\rm min}/(\mathrm{d.o.f.}) = 20.4/(19) \tag{4.20b}$$

for the four-parameter fit, and

$$\left.\begin{aligned} \bar{g}_Z^2(m_Z^2) &= 0.55525 - 0.00038\,\tfrac{\alpha_s'-0.1227}{0.0037} \pm 0.00059 \\ \bar{s}^2(m_Z^2) &= 0.23065 + 0.00003\,\tfrac{\alpha_s'-0.1227}{0.0037} \pm 0.00024 \end{aligned}\right\}$$
$$\rho_{\rm corr} = 0.24, \tag{4.21a}$$

$$\chi^2_{\rm min} = 20.4 + \left(\frac{\alpha_s' - 0.1227}{0.0037}\right)^2 + \left(\frac{\bar{\delta}_b + 0.0051}{0.0028}\right)^2, \tag{4.21b}$$

for the two-parameter fit with external α_s' and $\bar{\delta}_b$. The net effect of the low energy data is to move the mean value of $\bar{g}_Z^2(m_Z^2)$ down by 0.00032, i.e. nearly half a standard deviation. As can be seen from Fig. 7, this downward shift is mainly a consequence of the old ν_q–q scattering data [32].

Future results from the NUTEV Collaboration, succeeding to the CCFR Collaboration, are expected to improve considerably the constraints on the low energy form factors.

4.4 The (S,T,U)-fit

All neutral current data are summarized in (4.18) for low energy ($q^2 \approx 0$) and in (4.2) for the Z-shape parameters. In addition, the slightly improved W mass [6] in Table 1,

$$m_W = 80.356 \pm 0.125\,\mathrm{GeV} \tag{4.22}$$

gives

$$\bar{g}_W^2(0) = 0.4237 \pm 0.0013\,, \tag{4.23}$$

for $\bar{\delta}_G = 0.0055$ in (3.5).

Using (3.3) or (3.4) a three-parameter fit to all the electroweak data, i.e. the Z parameters, the W mass and the low-energy neutral-current data, is performed in terms of S, T, U, while α_s' and $\bar{\delta}_b$ are treated as external parameters. To be specific the top and Higgs masses required in the mild running of the charge form factors (see (3.8)) are set to 175 GeV and 100 GeV. The fit yields :

$$\left.\begin{aligned} S &= -0.33 - 0.056\,\tfrac{\alpha_s'-0.1227}{0.0037} + 0.06\,\tfrac{\delta_\alpha - 0.03}{0.09} \pm 0.13 \\ T &= 0.61 - 0.094\,\tfrac{\alpha_s'-0.1227}{0.0037} \qquad\qquad\qquad \pm 0.14 \\ U &= 0.48 + 0.069\,\tfrac{\alpha_s'-0.1227}{0.0037} + 0.02\,\tfrac{\delta_\alpha - 0.03}{0.09} \pm 0.38 \end{aligned}\right\}$$
$$\rho_{\rm corr} = \begin{pmatrix} 1 & 0.86 & -0.11 \\ & 1 & -0.21 \\ & & 1 \end{pmatrix}, \tag{4.24a}$$

$$\chi^2_{\rm min} = 20.3 + \left(\frac{\alpha_s' - 0.1227}{0.0037}\right)^2 + \left(\frac{\bar{\delta}_b + 0.0051}{0.0028}\right)^2, \quad (\mathrm{d.o.f.} = 21)\,. \tag{4.24b}$$

The dependence of the S and U parameters upon δ_α may be understood from (3.6) and (3.7). For an arbitrary value of $\bar{\delta}_G$ the parameter T should be replaced by $T' \equiv T + (0.0055 - \bar{\delta}_G)/\alpha$ [2]. Note that the uncertainty in S coming from $\delta_\alpha = 0.03 \pm 0.09$ [18] is of the same order as that from the uncertainty in from $\alpha_s = 0.118 \pm 0.003$ [28]; they are not at all negligible when compared to the overall error. The T parameter has little δ_α dependence, but is sensitive to α_s.

The above results, together with the SM predictions, are shown in Fig. 8 as the projection onto the (S, T) plane. Accurate parametrizations of the SM contributions to the S, T, U parameters are found in [2], while their compact parametrizations valid in the domain $160\,\mathrm{GeV} < m_t < 185\,\mathrm{GeV}$ and $40\,\mathrm{GeV} < m_H < 1000\,\mathrm{GeV}$ are given in (3.10). Also shown are the predictions [5] of the minimal (one-doublet) SU(N_c) Technicolor (TC) models with $N_c = 2, 3, 4$, where QCD-like spectra of Techni-bosons with the large N_c scaling and a specific top-quark mass generation mechanism is assumed. Obviously the current experiments provide a fairly stringent constraint on the simple TC models. Any TC model to be realistic must provide an additional negative contribution to S [34] and at the same time a rather small contribution to T. Our results confirm the observations [9,35] based on the previous data, and are consistent with those of other recent updates [36–38].

Table 5. Constraints on the parameters $S_{\rm new}$, $T_{\rm new}$, $U_{\rm new}$ which are obtained by subtracting the SM contribution $S_{\rm SM}$, $T_{\rm SM}$, $U_{\rm SM}$ from S, T, U for $\alpha_s = 0.118$ and $\delta_\alpha = 0.03$. Correlations among errors are the same as in (4.24a)

m_t (GeV)	m_H (GeV)	$\begin{pmatrix} S \\ T \\ U \end{pmatrix}$	$\chi^2_{\rm min}$/(d.o.f.)	$\begin{pmatrix} S_{\rm SM} \\ T_{\rm SM} \\ U_{\rm SM} \end{pmatrix}$	χ^2/(d.o.f.)	$\begin{pmatrix} S_{\rm new} \\ T_{\rm new} \\ U_{\rm new} \end{pmatrix}$
169	100	-0.27 ± 0.13 0.71 ± 0.14 0.41 ± 0.38	23.9/21 (30% CL)	-0.23 0.80 0.35	24.5/24 (43% CL)	-0.05 ± 0.13 -0.09 ± 0.14 0.06 ± 0.38
169	1000	-0.28 ± 0.13 0.70 ± 0.14 0.41 ± 0.38	23.9/21 (30% CL)	-0.07 0.51 0.34	57.5/24 (0.01% CL)	-0.21 ± 0.13 0.19 ± 0.14 0.07 ± 0.38
175	100	-0.26 ± 0.13 0.73 ± 0.14 0.39 ± 0.38	25.1/21 (24% CL)	-0.23 0.88 0.36	28.1/24 (26% CL)	-0.03 ± 0.13 -0.15 ± 0.14 0.03 ± 0.38
175	1000	-0.27 ± 0.13 0.72 ± 0.14 0.40 ± 0.38	25.1/21 (24% CL)	-0.08 0.58 0.36	48.4/24 (0.2% CL)	-0.20 ± 0.13 0.14 ± 0.14 0.04 ± 0.38
181	100	-0.25 ± 0.13 0.75 ± 0.14 0.38 ± 0.38	26.4/21 (19% CL)	-0.24 0.96 0.38	34.2/24 (8% CL)	-0.02 ± 0.13 -0.21 ± 0.14 0.00 ± 0.38
181	1000	-0.26 ± 0.13 0.74 ± 0.14 0.38 ± 0.38	26.5/21 (19% CL)	-0.08 0.66 0.37	41.3/24 (2% CL)	-0.18 ± 0.13 0.08 ± 0.14 0.01 ± 0.38

To be more quantitative Table 5 provides the values of S, T and U after subtracting the SM contributions ($S_{\rm new} \equiv S - S_{\rm SM}$, etc.). The m_t- and m_H-dependences of the extracted S, T and U values result from the fact that the SM prediction for $\bar{\delta}_b$ being strongly m_t dependent has been assumed in α'_s for a fixed $\alpha_s = 0.118$; see (4.10d) with $[\bar{\delta}_b]_{\rm NewPhysics} = 0$. All values in the table are obtained by setting $\alpha_s = 0.118$ and $\delta_\alpha = 0.03$. The values for different choices of α_s and δ_α together with the error correlation matrix can be read-off from (4.24). It is worth pointing out that the SM fit provides only a poor fit (less than 1% CL) when $m_H = 1000\,{\rm GeV}$ and $m_t < 170\,{\rm GeV}$. New physics contributions of *both* $S_{\rm new} \approx -0.2$ *and* $T_{\rm new} \approx 0.2$ may then be needed because of the large correlation of 0.86 between the two quantities. In fact, once $S_{\rm new}$ is given by a model of dynamical symmetry breaking, the $T_{\rm new}$ should be severely constrained by the data ; $T_{\rm new} - 1.1\,S_{\rm new} = 0.37 \pm 0.073$ for $m_t = 169\,{\rm GeV}$ and $m_H = 1000\,{\rm GeV}$. The necessity of an additional positive $T_{\rm new}$ contribution cannot easily be read off from Fig. 8, where the projection of the fit (4.24) onto the (S,T) plane is shown when the combination α'_s (4.1) of the Zb_Lb_L vertex form factor $\bar{\delta}_b$ and α_s are allowed to vary. The most stringent constraint on the S, T, U parameters is obtained as an eigenvector of the correlation matrix of (4.24):

$$T' - 1.10S' + 0.04U' = 0.99 \pm 0.073. \qquad (4.25)$$

Fit results for $S_{\rm new}$, $T_{\rm new}$ and $U_{\rm new}$ for other choices of m_t, m_H, α_s and δ_α can easily be obtained from the result (4.24) and the parametrization (3.10).

Finally, regarding the point $(S,T,U) = (0,0,0)$ as the one with no-electroweak corrections (a more precise treatment will be given in Sect. 5.2) $\chi^2_{\rm min}/({\rm d.o.f.}) = 141/(22)$ is found. On the other hand, if also the remaining electroweak corrections to G_F are switched off by setting $\bar{\delta}_G = 0$, then $T' = 0.0055/\alpha = 0.75$ is found and the point $(S,T',U) = (0,0.75,0)$ gives $\chi^2_{\rm min}/({\rm d.o.f.}) = 34.2/(22)$ being barely (5% CL) consistent with the data. As emphasized in [41], the genuine electroweak correction is not trivially established in this analysis because of the cancellation between the large T parameter from $m_t \sim 175$ GeV and the non-universal correction $\bar{\delta}_G$ to the muon decay constant in the observable combination [2] $T' = T + (0.0055 - \bar{\delta}_G)/\alpha$.

5 The minimal standard model confronting the electroweak data

Throughout this section all radiative corrections are assumed to be dominated by the SM contributions. Within the minimal SM all electroweak quantities are uniquely predicted as functions of m_t and m_H. A careful investigation is done to elucidate the role of the input parameters α_s and $\bar{\alpha}(m_Z^2)$ required for the interpretation.

A brief discussion on the significance of bosonic radiative corrections containing the weak-boson self-couplings is also given.

5.1 4-parameter fit

Within the Minimal Standard Model the electroweak precision data are expressed in terms of the two mass parameters m_t and m_H. In a first, and most general, attempt

also the parameters α_s and δ_α are left free. The result of the 4-parameter fit yields :

$$\left.\begin{aligned} m_t(\,\mathrm{GeV}) &= 151 \pm 13 \\ x_H \quad &= -0.5 \pm 1.5 \\ \alpha_s \quad &= 0.1198 \pm 0.0031 \\ \delta_\alpha \quad &= 0.13 \pm 0.34 \end{aligned}\right\}$$

$$\rho_{\rm corr} = \begin{pmatrix} 1.0 & 0.0 & -0.0 & 0.5 \\ & 1.0 & -0.1 & -0.8 \\ & & 1.0 & 0.1 \\ & & & 1.0 \end{pmatrix}, \tag{5.1a}$$

$$\chi^2_{\rm min}/(\text{d.o.f.}) = 21.9/(21)\,. \tag{5.1b}$$

Instead of fitting m_H itself it is more appropriate to fit $x_H = \log(m_H/100\,\mathrm{GeV})$; otherwise the uncertainties are too asymmetric. It is remarkable that the fitted α_s value agrees well with the global fit result [28] and that its uncertainty is as low as 0.003. Also the fitted $\bar\alpha(m_Z^2)$ agrees within the large errors with other recent measurements [16–19]. The fitted m_t value is about 2-σ below the present Tevatron measurement, $m_t = 175 \pm 6\,\mathrm{GeV}$ [8]. The relatively low m_H value, $m_H = 60^{+210}_{-50}\,\mathrm{GeV}$, is a consequence of this. m_H and δ_α appear to be strongly anti-correlated as a consequence of the strong asymmetry constraint which is sensitive to δ_α. Large δ_α (large $1/\bar\alpha(m_Z^2)$) implies small m_H.

Next we present results of the 4-parameter fit on the electroweak data when external constraints on α_s, $\alpha_s = 0.118 \pm 0.003$ [28], and those on δ_α are imposed. For $\delta_\alpha = 0.03 \pm 0.09$ [18], we obtain

$$\left.\begin{aligned} m_t(\,\mathrm{GeV}) &= 153 \pm 10 \\ x_H \quad &= -0.8 \pm 0.8 \\ \alpha_s \quad &= 0.1190 \pm 0.0022 \\ \delta_\alpha \quad &= 0.04 \pm 0.09 \end{aligned}\right\}$$

$$\rho_{\rm corr} = \begin{pmatrix} 1.0 & 0.6 & -0.1 & 0.3 \\ & 1.0 & -0.1 & -0.3 \\ & & 1.0 & 0.1 \\ & & & 1.0 \end{pmatrix}, \tag{5.2a}$$

$$\chi^2_{\rm min}/(\text{d.o.f.}) = 22.2/(23)\,, \tag{5.2b}$$

while for $\delta_\alpha = 0.12 \pm 0.06$ [16], we obtain

$$\left.\begin{aligned} m_t(\,\mathrm{GeV}) &= 151 \pm 11 \\ x_H \quad &= -0.5 \pm 0.8 \\ \alpha_s \quad &= 0.1189 \pm 0.0022 \\ \delta_\alpha \quad &= 0.12 \pm 0.06 \end{aligned}\right\}$$

$$\rho_{\rm corr} = \begin{pmatrix} 1.00 & 0.8 & -0.1 & 0.1 \\ & 1.0 & -0.0 & -0.2 \\ & & 1.0 & 0.0 \\ & & & 1.0 \end{pmatrix}, \tag{5.3a}$$

$$\chi^2_{\rm min}/(\text{d.o.f.}) = 22.1/(23)\,. \tag{5.3b}$$

Because of the strong correlation between x_H and δ_α in (5.1), the error of x_H is reduced by about a factor of two. At the same time, a strong positive correlation between the errors of m_t and x_H appears. Larger δ_α (smaller $\bar\alpha(m_Z^2)$) implies larger x_H and larger m_t. The fitted m_t value is still somewhat smaller than the observed Tevatron value [8]. This is partly due to the average R_b value, which is presently about 2-σ larger than the SM prediction assuming $m_t = 175\,\mathrm{GeV}$. The fit (5.2) without R_b and R_c data yields

$$\left.\begin{aligned} m_t(\,\mathrm{GeV}) &= 158 \pm 12 \\ x_H \quad &= -0.5 \pm 1.0 \\ \alpha_s \quad &= 0.1188 \pm 0.0022 \\ \delta_\alpha \quad &= 0.03 \pm 0.09 \end{aligned}\right\}$$

$$\rho_{\rm corr} = \begin{pmatrix} 1.0 & 0.8 & -0.1 & 0.1 \\ & 1.0 & -0.0 & -0.4 \\ & & 1.0 & 0.0 \\ & & & 1.0 \end{pmatrix}, \tag{5.4a}$$

$$\chi^2_{\rm min}/(\text{d.o.f.}) = 20.5/(22)\,. \tag{5.4b}$$

The discrepancy is now reduced to the 1-σ level. Although the above elliptic parametrizations reproduce the χ^2 function only approximately, we find that the preferred ranges of m_t and m_H in (5.4) agree well with the corresponding results of [39].

Throughout (5.1)–(5.4), the fitted α_s value agree well with the global average, $\alpha_s = 0.118 \pm 0.003$ [28]. A slightly smaller value of m_H ($\sim 50\,\mathrm{GeV}$) is favored with the error of order 1 for $\log m_H$, and slightly smaller value of m_t is favored as compared to the Tevatron measurement. The best-fit value of m_H is sensitive to δ_α, whereas that of m_t is sensitive to the R_b data. The 4-parameter fit results given in (5.1)–(5.4) are intended to illustrate qualitatively our understanding of the SM fit to the electroweak. The errors are not fully elliptic. More accurate constraints on these parameters can be obtained from the parametrization of the χ^2-function given below in (5.5).

In conclusion, the fits are stable and agree with the a priori knowledge on α_s and δ_α. It is justified to proceed with an in-depth study based on the two parameters m_t and m_H, where now α_s and δ_α play the role of external parameters.

5.2 Constraints on m_t and m_H as functions of α_s and $\bar\alpha(m_Z^2)$

In the minimal SM all relevant form factor values, i.e. $\bar g_Z^2(m_Z^2)$, $\bar s^2(m_Z^2)$, $\bar g_Z^2(0)$, $\bar s^2(0)$, $\bar g_W^2(0)$ and $\bar\delta_b(m_Z^2)$, are predicted uniquely in terms of on the two mass parameters m_t and m_H. A convenient parametrization of the SM contributions to these form factors is given in (3.6)–(3.10), as functions of $x_t = (m_t(\,\mathrm{GeV}) - 175)/10$, $x_H = \log(m_H(\,\mathrm{GeV})/100)$ together with α_s and δ_α. Figure 9 shows the result of the fit to all electroweak data in the (m_H, m_t)-plane for choices of α_s and δ_α representative of

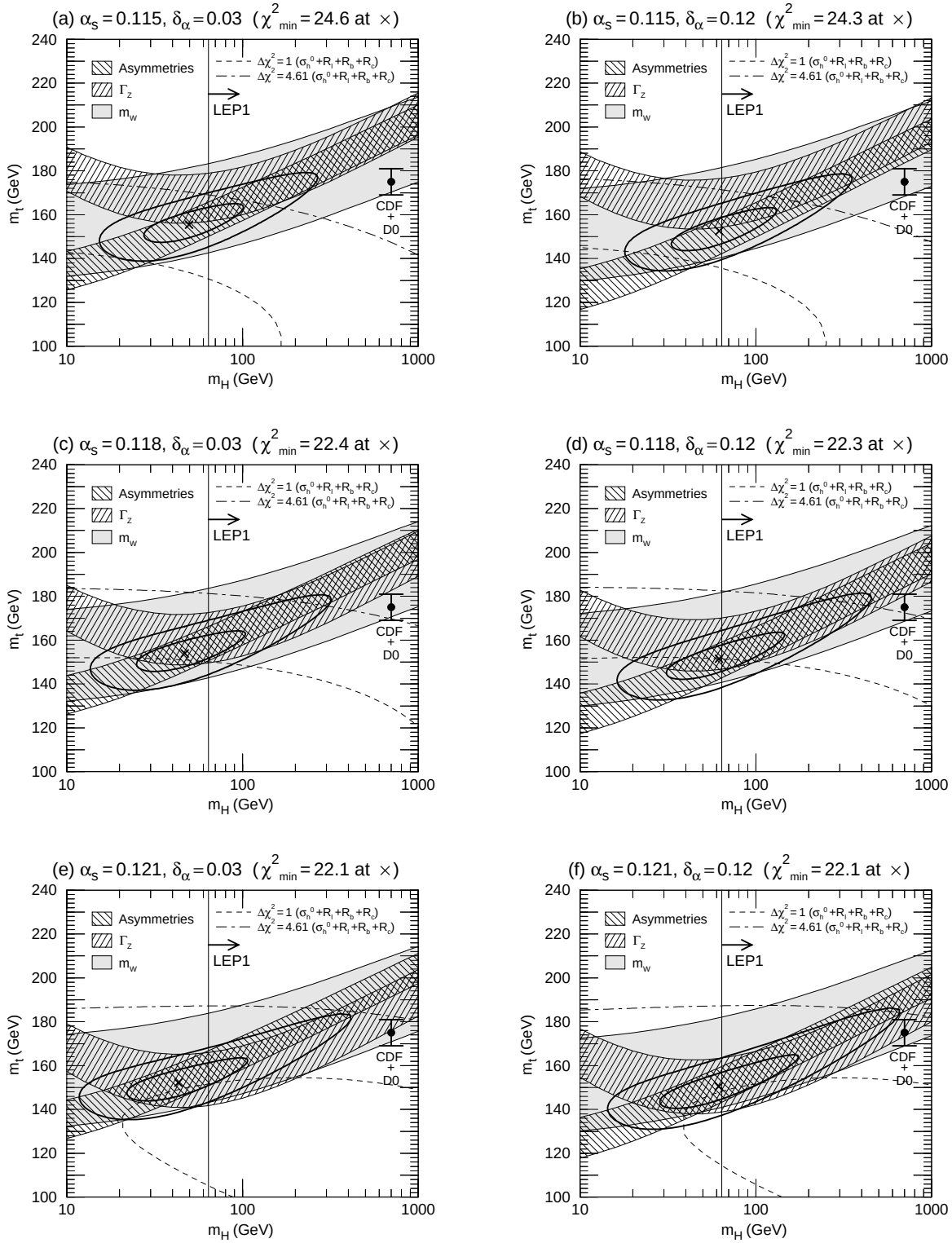

Fig. 9. The SM fit to all electroweak data in the $(m_H,\, m_t)$ plane for various choices of $(\alpha_s, \delta_\alpha)$: **a** (0.115,0.03) , **b** (0.115,0.012) , **c** (0.118,0.03) , **d** (0.118,0.012) , **e** (0.121,0.03) , **f** (0.121,0.012) , where $\delta_\alpha = 1/\bar{\alpha}(m_Z^2) - 128.72$ [2]. The *thick inner* and *outer contours* correspond to $\Delta\chi^2 = 1$ ($\sim 39\%$ CL), and $\Delta\chi^2 = 4.61$ ($\sim 90\%$ CL), respectively. The minimum of χ^2 is marked by the sign "×". Also shown are the 1-σ bands from the Z-pole asymmetries, Γ_Z and m_W. The *dashed lines* show the constraint from the sum of σ_h^0, R_ℓ, R_b and R_c

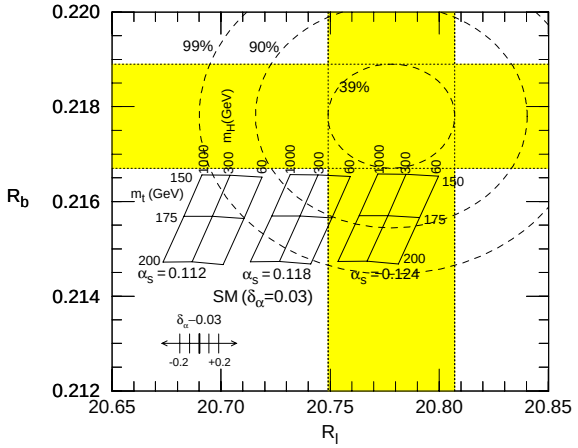

Fig. 10. The R_b vs R_ℓ plane. The SM predictions are shown in the range $120\,\mathrm{GeV} < m_t < 240\,\mathrm{GeV}$, and $60\,\mathrm{GeV} < m_H < 1\,\mathrm{TeV}$, for three cases of α_s (α_s=0.11, 0.12 and 0.13). These predictions are for $\delta_\alpha = 0.03$, and their dependences on δ_α are also indicated. Also shown are the 39%, 90% and 99% CL contours obtained by combining only the R_ℓ and R_b data

their present knowledge. The figure exhibits to what extent the best-fit values as well as the size and orientation of the corresponding error ellipses ($\Delta\chi^2 \equiv \chi^2 - \chi^2_{\rm min} =$ 1 and 4.61) depend on the knowledge of the external parameters α_s and δ_α.

In order to understand how the fit comes about the 1-σ constraints from the individual observables are shown separately. The narrow "asymmetry" band is sensitive to δ_α, whereas the "Γ_Z" band is sensitive to α_s. The asymmetries constrain m_t and m_H through $\bar{s}^2(m_Z^2)$, while Γ_Z does so through all the three form factors $\bar{g}_Z^2(m_Z^2)$, $\bar{s}^2(m_Z^2)$ and $\bar{\delta}_b(m_Z^2)$. It is most remarkable [3] that in the SM Γ_Z depends upon almost the same combination of m_t and m_H as the one measured through $\bar{s}^2(m_Z^2)$ provided m_H is larger than about 60 GeV, which is indeed the range not excluded by the LEP1 experiments. The reason can be traced back to the approximate cancellation of the quadratic m_t-dependence of $\bar{g}_Z^2(m_Z^2)$ and $\bar{\delta}_b$. Thus, the asymmetries and Γ_Z alone, despite their quite small experimental errors, are constraining only a narrow band in the (m_t,m_H)-plane. The present constraint due to the m_W measurement overlaps this band.

Additional information is required to disentangle the above m_t-m_H correlation. This is provided by R_ℓ, σ_h, R_b and is shown in Fig. 9 by dashed lines corresponding to a $\Delta\chi^2$ of 1 (∼39% CL) and 4.61 (∼90% CL). The constraints due to R_ℓ and R_b can also be seen in Fig. 10. R_ℓ is sensitive to the assumed value of α_s, and, for $\alpha_s = 0.118$, the data favors small m_H. R_b is neither sensitive to α_s nor m_H and the present average disfavors large m_t.

Without the data on R_ℓ, σ_h and R_b the region of large m_H-values in the (m_t, m_H)-band of Fig. 9 ($m_H \sim 1\,\mathrm{TeV}$) would not be excluded at all, as far as the electroweak data are concerned. It is worth noting that in comparing Fig. 9 (a) with (e) (or (b) with (f)) the Γ_Z-band is shifted downwards by more than 10 GeV in the top quark mass when one increases α_s from 0.115 to 0.121, but despite of this shift the best-fit point moves only marginally downwards by about 1.7 GeV (see also the parametrization (5.5b) below). This is mainly because the constraint from σ_h^0, R_ℓ and R_b allows larger m_t for larger α_s, as can be seen from dashed contours in Fig. 9, or from Fig. 10. The fit improves slightly at larger α_s, because the Γ_Z constraint then favors lower m_t which in turn is favored by the R_b data. On the other hand the change in δ_α from the mean value of the estimate of [18], 0.03, to that of [16], 0.12, lowers the best-fit m_t value by about 5 GeV and enhances that of m_H slightly (by about 15 GeV), whereas the overall fit quality remains unchanged. The χ^2 function of the fit to all electroweak data can be parametrized in terms of the four parameters m_t, m_H, α_s and δ_α :

$$\chi^2_{\rm SM}(m_t, m_H, \alpha_s, \delta_\alpha) = \left(\frac{m_t - \langle m_t\rangle}{\Delta m_t}\right)^2 + \chi^2_H(m_H, \alpha_s, \delta_\alpha)\,, \quad (5.5a)$$

with

$$\langle m_t\rangle = 162.4 + 13.0\,\log\frac{m_H}{100} + 0.8\,\log^2\frac{m_H}{100} - 0.85\left(\frac{\alpha_s - 0.118}{0.003}\right) - 4.9\left(\frac{\delta_\alpha - 0.03}{0.09}\right), \quad (5.5b)$$

$$\Delta m_t = 5.5 - 0.06\,\log\frac{m_H}{100} - \left(0.090 - 0.018\,\log\frac{m_H}{100}\right)\frac{m_t - 175}{6}\,, \quad (5.5c)$$

and

$$\chi^2_H(m_H, \alpha_s, \delta_\alpha) = 22.1 + \left(\frac{\delta_\alpha - 0.19}{0.18}\right)^2 + \left(\frac{\alpha_s - 0.1201 + 0.0011\,\delta_\alpha}{0.0031}\right)^2 - \left(\frac{\alpha_s - 0.1343 + 0.063\,\delta_\alpha}{0.0071}\right)\log\frac{m_H}{100} - \left(\frac{\alpha_s - 0.1305}{0.0129}\right)\log^2\frac{m_H}{100}\,. \quad (5.5d)$$

Here m_t and m_H are measured in GeV, and d.o.f. = 25. This parametrization reproduces the exact χ^2 function within a few percent accuracy in the range $100\,\mathrm{GeV} < m_t < 250\,\mathrm{GeV}$, $60\,\mathrm{GeV} < m_H < 1000\,\mathrm{GeV}$ and $0.10 < \alpha_s(m_Z) < 0.13$. The best-fit value of m_t for a given set of m_H, α_s and δ_α is readily obtained from (5.5b) with its approximate error of (5.5c). See dotted curves in Fig. 11.

For $m_H = 60, 300, 1000\,\mathrm{GeV}$, $\alpha_s = 0.118 \pm 0.03$ and $\delta_\alpha = 0.03 \pm 0.09$, one obtains

$$m_t = 178 \pm 6^{+19(m_H=1000)}_{-21(m_H=60)} \mp 1(\alpha_s) \mp 5(\delta_\alpha)\,, \quad (5.6)$$

where the mean value is for $m_H = 300$ GeV. The fit (5.6) agrees with the best value from CDF and D0

$$m_t = 175 \pm 6\ \ \mathrm{GeV}. \quad (5.7)$$

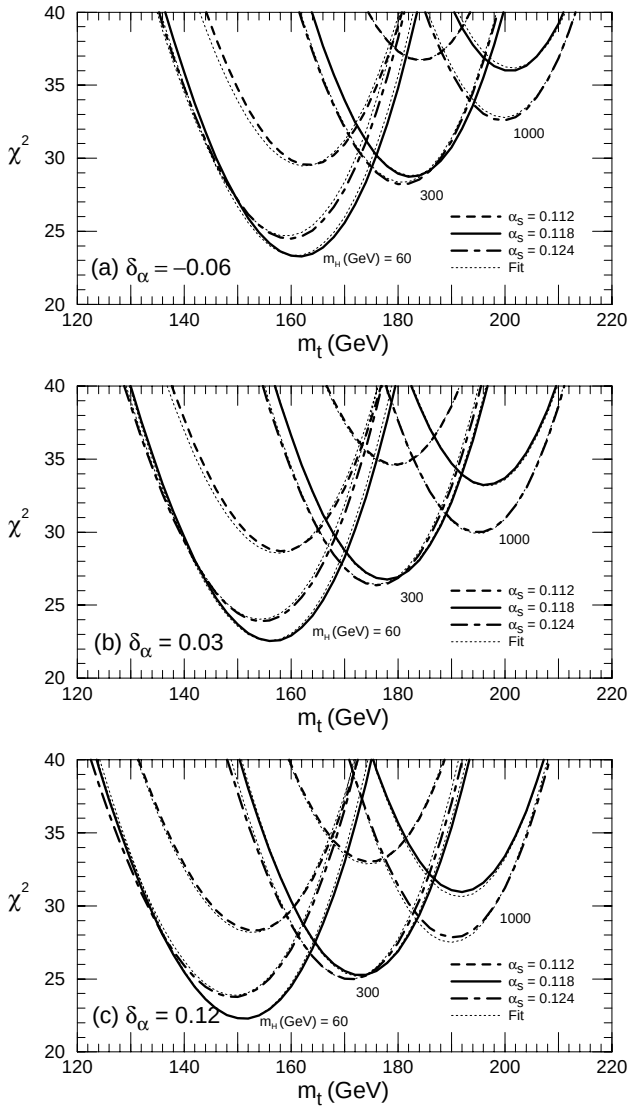

Fig. 11. Total χ^2 of the SM fit to all the electroweak data as functions of m_t for $m_H = 60$, 300, 1000 GeV and $\alpha_s(m_Z) = 0.112$, 0.118, 0.124. The uncertainty δ_α in the hadronic vacuum polarization contribution to the effective charge $1/\bar{\alpha}(m_Z^2)$ is shown for three cases, $\delta_\alpha = -0.06$ **a**, 0.03 **b**, +0.12 **c**. The *dotted lines* are obtained by using the approximate formula (5.5). The number of degrees of freedom is 25

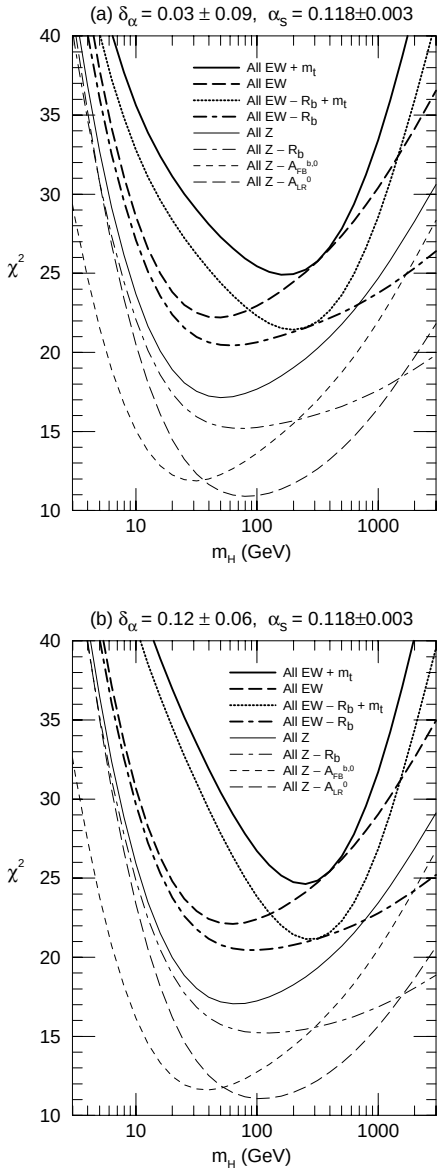

Fig. 12. Total χ^2 of the SM fit to all the electroweak data as functions of m_H when m_t is allowed to vary, with $\alpha_s(m_Z) = 0.118 \pm 0.003$ [28] for $\delta_\alpha = 0.03 \pm 0.09$ [18] **a** and $\delta_\alpha = 0.12 \pm 0.06$ [16] **b**. Results for various sets of the electroweak data with or without the Tevatron m_t data, $m_t = 175 \pm 6$ GeV [8] are given. The degrees of freedom is 25 for 'All EW $+m_t$' case

This agreement strongly suggests that the electroweak theory respects the gauge invariance, since otherwise the quantum corrections could not be calculated. An elaboration on this point follows in the next subsection. Furthermore, the successful prediction of m_t based on the simple SM radiative corrections strongly supports the presence of the custodial SU(2) symmetry as part of physics responsible for spontaneous symmetry breaking. Without custodial SU(2) there would have been no prediction for m_t. Furthermore, the mechanism that leads to the large mass splitting of the third generation quarks should give rise to a T value which is similar to its standard model value. Therefore, the success of the SM prediction not only suggests the presence of the custodial SU(2) symmetry, but also constrains the mechanism of the fermion mass generation.

Due to the quadratic form of (5.5) one can readily integrate out the unwanted terms, for instance those containing α_s and/or δ_α, and render the result independent of them. Also, additional constraints on the external parameters α_s and δ_α, such as those from future improved measurements or the constraint from the grand unification of these couplings may be added without difficulty.

As discussed above, the value for m_H resulting from the Standard Model fit is correlated with the value of mt.

The present value for R_b which disfavors large masses of the top quark induces therefore a small value of the Higgs mass. It should also be noted that the choice of the value of α_s as an external parameter implies via (4.2) a constraint on the vertex form factor $\bar{\delta}_b$ and influences in turn the fit value for m_H. Shown in Fig. 12 are the m_H-dependence of χ^2 under various assumptions. We present in Table 6 the corresponding 95% CL upper and lower bounds on m_H(GeV) from the electroweak data. A low mass Higgs boson is clearly favored. However, this trend disappears for $\alpha_s = 0.118 \pm 0.003$ [28], once we ignore the R_b data. If we adopt the estimate $\delta_\alpha = 0.03 \pm 0.09$ [18] for $\bar{\alpha}(m_Z^2)$, the 95% CL upper bound on m_H is 270 GeV from all the Z boson data, while it weakens to 1200 GeV, if the R_b data are ignored. The corresponding upper bounds with the estimate $\delta_\alpha = 0.12 \pm 0.06$ [16] are 370 GeV and 1900 GeV, respectively. An addition of the low energy neutral current data slightly lowers the upper m_H bound, mainly because the combined fit, (4.19), gives slightly smaller $\bar{g}_Z^2(m_Z^2)$, i.e. smaller T, than the Z parameters would give alone. Just like smaller R_b favors smaller m_t, smaller T favors smaller m_t and through the strong m_t and m_H correlation from the Γ_Z and the asymmetry data smaller m_H is favored. It is hence the direct measurement from the Tevatron, $m_t = 175 \pm 6$ GeV, that essentially constrains the allowed m_H, $m_H < 480$ GeV for $\delta_\alpha = 0.03 \pm 0.12$ or $m_H < 590$ GeV for $\delta_\alpha = 0.09 \pm 0.06$ at 95% CL, given the Γ_Z and the asymmetry constraint.

The constraints on m_H become much stronger once the top quark mass is known precisely, either due to more precise measurements or due to deeper theoretical insight. Lower and upper bounds on m_H are shown in Fig. 13 and in Table 7 as functions of m_t for the two estimates of $\bar{\alpha}(m_Z^2)$. With the estimate of E-J [18], $\delta_\alpha = 0.03 \pm 0.12$, a lower m_H is favored ($m_H < 360$ GeV at 95% CL), if $m_t < 170$ GeV, while an intermediate m_H is favored ($m_H > 140$ GeV at 95% CL) for $m_t > 180$ GeV. With the estimate of M-Z [16], $\delta_\alpha = 0.12 \pm 0.06$, similar constraints are found at about 5 GeV smaller m_t. It is hence rather crucial for models where the Higgs boson is light (e.g. $m_H < 130$ GeV in the MSSM [42]) to have m_t smaller than the actual present mean value, $m_t \sim 175$ GeV.

Finally, we repeat the 4-parameter fits, (5.1)–(5.3) on the electroweak data when the direct m_t measurement, $m_t = 175 \pm 6$ GeV (Tevatron), is taken into account. Without external constraints on α_s and δ_α, we find

$$\left.\begin{aligned} m_t(\,\mathrm{GeV}) &= 173 \pm 6 \\ x_H \quad &= 1.7 \pm 1.1 \\ \alpha_s \quad &= 0.1218 \pm 0.0037 \\ \delta_\alpha \quad &= 0.30 \pm 0.26 \end{aligned}\right\}$$

$$\rho_{\mathrm{corr}} = \begin{pmatrix} 1.0 & 0.4 & 0.2 & -0.1 \\ & 1.0 & 0.5 & -0.9 \\ & & 1.0 & -0.4 \\ & & & 1.0 \end{pmatrix}, \tag{5.8a}$$

$$\chi^2_{\mathrm{min}}/(\mathrm{d.o.f.}) = 23.8/(22)\,. \tag{5.8b}$$

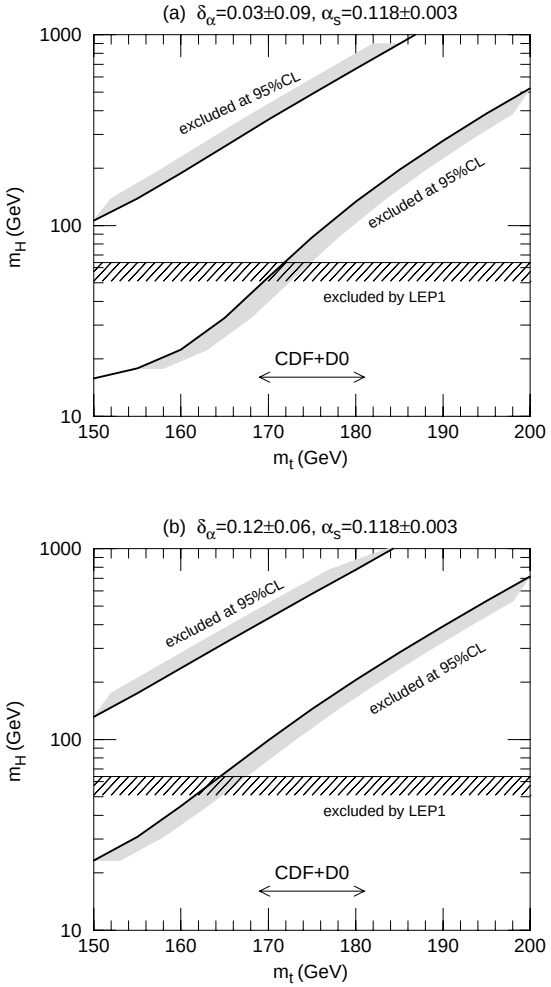

Fig. 13. Constraints on the Higgs mass in the SM from all the electroweak data. Upper and lower bounds of the Higgs mass at 95% CL are shown as functions of the top mass m_t, where m_t is treated as an external parameter with negligible uncertainty. The results are shown for $\alpha_s = 0.118 \pm 0.003$ [28] and for $\delta_\alpha = 0.03 \pm 0.09$ [18] **a** and $\delta_\alpha = 0.12 \pm 0.06$ [16] **b**. Also shown are the direct lower bound on m_H from LEP1 and the Tevatron data $m_t = 175 \pm 6$ GeV [8]

The top quark mass appears now basically determined by the direct measurement, while the mean δ_α grows considerably and, consequently, a larger m_H, $m_H = 530^{+1600}_{-170}$ GeV is favored. The shifted best value of m_t slightly affects the sensitivity to α_s (see (5.1)). The value of $\alpha(m_Z^2)$ obtained from the electroweak measurements agrees roughly with that of [37], which may be expressed as $\delta_\alpha = 0.21^{+0.25}_{-0.32}$.

Adding the external constraint $\alpha_s = 0.118 \pm 0.003$ [28] does not significantly alter the situation, because the fit (5.8) results in the α_s value consistent with the world average.

Because the best-fit value of δ_α in (5.8) is slightly larger than the estimate $\delta_\alpha = 0.03 \pm 0.09$ by E-J [18], the strong negative correlation between $\Delta\delta_\alpha$ and Δx_H in (5.8) entails

Table 6. 95% CL upper and lower bounds of m_H(GeV) for $\alpha_s = 0.118 \pm 0.003$ [28], $\delta_\alpha = 0.03 \pm 0.09$ [18] or $\delta_\alpha = 0.12 \pm 0.06$ [16]. Results for various sets of the electroweak data with or without the Tevatron m_t data, $m_t = 175 \pm 6\,\mathrm{GeV}$ [8] are given

	$\alpha_s = 0.118 \pm 0.003$							
	$\delta_\alpha = 0.03 \pm 0.12$				$\delta_\alpha = 0.12 \pm 0.06$			
	best-fit	lower bound	upper bound	$\chi^2_{\min}$	best-fit	lower bound	upper bound	$\chi^2_{\min}$
EW + m_t	170	46	480	24.9	240	87	590	24.6
EW + m_t − R_b	200	54	550	21.4	280	100	670	21.1
EW	51	17	270	17.1	67	21	370	17.1
EW − R_b	60	17	730	20.4	90	22	1200	20.4
Z	51	17	270	17.1	67	21	370	17.1
Z − R_b	72	18	1200	15.2	120	24	1900	15.2
Z − $A^{b,0}_{\mathrm{FB}}$	30	11	140	11.9	38	13	200	11.6
Z − A^{0}_{LR}	82	23	450	10.9	110	29	590	11.1

Table 7. 95% CL upper and lower bounds of m_H(GeV) when m_t is fixed externally. Two estimates of $\bar{\alpha}(m_Z^2)$ are examined, $\delta_\alpha = 0.03 \pm 0.09$ [18] and $\delta_\alpha = 0.12 \pm 0.06$ [16], for $\alpha_s = 0.118 \pm 0.003$ [28]

	$\alpha_s = 0.118 \pm 0.003$							
	$\delta_\alpha = 0.03 \pm 0.09$				$\delta_\alpha = 0.12 \pm 0.06$			
m_t	best-fit	lower bound	upper bound	$\chi^2_{\min}$	best-fit	lower bound	upper bound	$\chi^2_{\min}$
160	72	22	190	22.7	110	45	240	22.6
165	110	33	260	23.4	150	67	320	23.3
170	150	54	360	24.3	220	99	430	24.0
175	220	87	490	25.3	300	140	580	24.9
180	310	130	660	26.4	410	210	780	26.0
185	430	200	900	27.6	550	290	1000	27.1
190	590	280	1200	28.9	740	390	1400	28.5

a sizeably lower m_H:

$$\left.\begin{aligned} m_t(\,\mathrm{GeV}) &= 171 \pm 6 \\ x_H &= 0.5 \pm 0.6 \\ \alpha_s &= 0.1191 \pm 0.0022 \\ \delta_\alpha &= 0.05 \pm 0.08 \end{aligned}\right\}$$

$$\rho_{\mathrm{corr}} = \begin{pmatrix} 1.0 & 0.6 & 0.1 & -0.0 \\ & 1.0 & 0.2 & -0.6 \\ & & 1.0 & -0.1 \\ & & & 1.0 \end{pmatrix}, \tag{5.9a}$$

$$\chi^2_{\min}/(\mathrm{d.o.f.}) = 24.9/(24)\,. \tag{5.9b}$$

Since the four parameter fits are not fully elliptic, we show in Fig. 14 both the 1-σ and 90% CL allowed regions in the (m_H, m_t) plane by solid contours. The 1-σ preferred range $m_H = 170^{+150}_{-90}\,\mathrm{GeV}$ agrees roughly with the estimates of [1,39,40]. Similar results with slightly larger m_H are found, if we adopt the M-Z estimation [16] $\delta_\alpha = 0.12 \pm 0.06$:

$$\left.\begin{aligned} m_t(\,\mathrm{GeV}) &= 172 \pm 6 \\ x_H &= 0.9 \pm 0.6 \\ \alpha_s &= 0.1193 \pm 0.0022 \\ \delta_\alpha &= 0.12 \pm 0.06 \end{aligned}\right\}$$

$$\rho_{\mathrm{corr}} = \begin{pmatrix} 1.0 & 0.7 & 0.1 & -0.0 \\ & 1.0 & 0.2 & -0.4 \\ & & 1.0 & -0.1 \\ & & & 1.0 \end{pmatrix}, \tag{5.10a}$$

$$\chi^2_{\min}/(\mathrm{d.o.f.}) = 24.6/(24)\,. \tag{5.10b}$$

The corresponding allowed ranges in the (m_H, m_t) plane are given by dashed contours in Fig. 14. The preferred m_H range is now $m_H = 240^{+180}_{-110}\,\mathrm{GeV}$. We note here that once the external m_t data is included in the fit, the relative importance of the R_b on the SM fit decreases. The above fit (5.9) and (5.10) are barely affected by excluding the R_b data.

The above exercises demonstrate well the overall consistency of the electroweak radiative corrections in the SM and emphasize at the same time the importance of an improved $\bar{\alpha}(m_Z^2)$ estimate for constraining m_H in fits based on electroweak precision experiments.

5.3 Is there already indirect evidence for the standard W self-coupling?

The success of the SM in describing all precision electroweak experiments at the quantum level may be taken

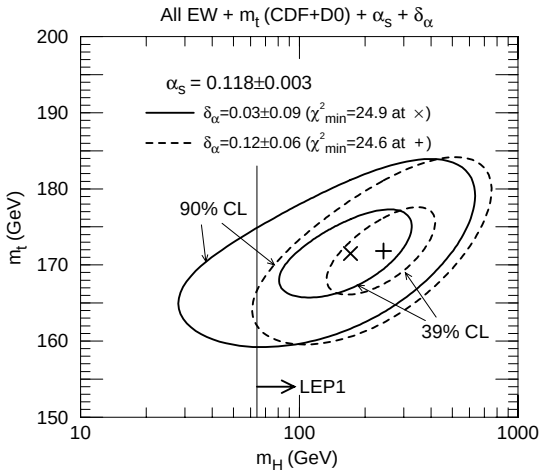

Fig. 14. The SM fit to all electroweak data in the (m_H, m_t) plane with external constraints on m_t from Tevatron, $m_t = 175 \pm 6\,\mathrm{GeV}$ [8], $\alpha_s = 0.118 \pm 0.003$ [28], and two estimates [16, 18] for $\delta_\alpha = 1/\bar{\alpha}(m_Z^2) - 128.72$. The *inner* and *outer contours* correspond to $\Delta\chi^2 = 1$ ($\sim$ 39% CL), and $\Delta\chi^2 = 4.61$ ($\sim$ 90% CL), respectively. The minimum of χ^2 is marked by the sign "$\times$" for the $\bar{\alpha}(m_Z^2)$ estimate of [18] and by the sign "+" for the estimate [16]. Also shown is the direct lower bound on m_H from LEP1

as indirect evidence of the non-Abelian nature of the electroweak theory, or respectively of the standard universal gauge-boson self-couplings, because it is the non-Abelian gauge symmetry of the SM which ensures its renormalizability.

Any alternative [43] to gauge models should necessarily have the new physics (cut-off) scale of order m_W, whereas the universality of the weak interactions may be associated with the underlying symmetry of the fundamental theory and the vector boson dominance which require relatively high ($\gg m_W$) scales for new physics. The fact that the SM works well at the quantum level indicates that the weak boson interactions do not deviate significantly from their gauge theory form at least up to the scale of $2m_t$. Therefore, it is instructive to study in more detail which part of the standard radiative corrections is supported by experiment and whether indeed there is evidence for the gauge boson self-couplings.

It is not straightforward to answer this question, since we have to identify which finite portion of the quantum corrections is sensitive to the weak-boson self-interactions. Usually one splits the complete SM radiative corrections into just two separately gauge invariant pieces, namely the fermionic loop contributions to the gauge-boson self-energies and the rest. It can then be stated unambiguously that neither of the corrections alone is sufficient to describe the data, and that only the inclusion of both contributions ensures the success of the SM radiative corrections [44]. As a matter of fact, the bosonic part of the correction contains the weak boson self-interactions as an essential part and in this sense it is indirect evidence for universal couplings.

In a more detailed attempt [45] at understanding the importance of bosonic contributions due to the WWZ and $WW\gamma$ couplings, it should be elucidated to what extent these finite bosonic correction terms depend on the splitting of the gauge bosons into themselves. For instance, the box diagrams do not contain gauge-boson self-couplings. It is useful to split the bosonic corrections into three separately gauge-invariant pieces, namely 'box-like', 'vertex-like' and 'propagator-like' pieces by appealing to the S-matrix pinch technique [10]. It is then only the 'vertex-like' and 'propagator-like' pieces which contain the gauge boson self-couplings. Schematically we separate the SM radiative corrections into the following five pieces:

$\mathcal{M} =$ QED/QCD (A)
+ fermion-loop (B)
+ box (C)
+ vertex (D)
+ bosonic-loop (E) (5.11)

Details of this separation for each radiative correction term may be obtained straightforwardly from the analytic expressions presented in [2]. By confronting these 'predictions' with the electroweak data the results of Table 8 are obtained.

The 'no-EW' entry confronts the tree-level predictions of the SM where only QCD and external QED corrections (A) are applied. In this column $\bar{\alpha}(m_Z^2)$ is calculated by including only contributions from light quarks and leptons with $\delta_h = 0.03$ [2,18] for the hadronic uncertainty. It is quite striking to re-confirm the observation [41] that these 'no-EW' predictions agree well with experiments at LEP1/SLC. In fact, it reduces the χ^2 over the SM, partly because of the R_b data, which prefer no electroweak corrections $\bar{\delta}_b(m_Z^2) = 0$ compared to the SM prediction $\bar{\delta}_b(m_Z^2) = -0.00995$ for $m_t = 175\,\mathrm{GeV}$. It is only the m_W value [46] and the Z boson width which give significantly higher χ^2 compared to the SM.

This can be understood as follows [45]. The three most accurately constrained electroweak parameters are $\bar{s}^2(m_Z^2)$ from the asymmetries, $\bar{g}_Z^2(m_Z^2)$ from Γ_Z at LEP1/SLC experiments, and m_W from Tevatron experiments. In terms of the 'observable' combinations (S', T', U') of (3.7), they can be expressed as

$$\bar{g}_Z^2(0) \approx 0.5456 + 0.0040T' \tag{5.12a}$$
$$\bar{s}^2(m_Z^2) \approx 0.2324 + 0.0036S' - 0.0024T' \tag{5.12b}$$
$$m_W(\,\mathrm{GeV}) \approx 79.84 - 0.28S' + 0.42T' + 0.33U' - 0.29(T' - T)\,. \tag{5.12c}$$

In the absence of electroweak corrections, the predictions are obtained by setting $S = T = U = \bar{\delta}_G = 0$ and also

by setting $\bar{g}_Z^2(m_Z^2) - \bar{g}_Z^2(0) = 0$. The purely light flavor value of $1/\bar{\alpha}(m_Z^2) = 1/\alpha(m_Z^2)_{\rm l.f.} = 128.89$ (see Table 4) corresponds to $\bar{\delta}_\alpha = 0.17$. These input values give rise to $(S', T', U') = (-0.12, 0.75, -0.04)$ which is not far from their SM values $(-0.23, 0.88, 0.36)$ for $m_t = 175\,\mathrm{GeV}$, $m_H = 100\,\mathrm{GeV}$ and $\bar{\delta}_G = 0.0055$, or from the (S, T, U) fit result of (4.24). The 'no-EW' case thus gives almost the same predictions for the three charge form factors, $\bar{g}_Z^2(0)$, $\bar{s}^2(m_Z^2)$, and $\bar{g}_W^2(0)$ with those of the SM. All the asymmetry data at LEP1/SLC are hence reproduced well. The low energy neutral current experiments are also reproduced well, since the running of the $\bar{s}^2(q^2)$ charge below the m_Z scale is essentially governed by the 'QED' effects. The 'no-EW' model predicts significantly smaller Γ_Z by about 3 to 4 σ for $\alpha_s = 0.118 \pm 0.003$, because the running of the $\bar{g}_Z^2$ charge, $\bar{g}_Z^2(m_Z^2) - \bar{g}_Z^2(0) \sim 0.05$ has been ignored. Furthermore, it fails to predict the measured m_W-value by about 3 σ, because its prediction is sensitive directly to the μ decay correction factor $\bar{\delta}_G$ in (3.5). This results in the last term in (5.12c), $-0.29(T' - T)$, which lowers the m_W prediction by more than 300 MeV.

The next '+fermion' column[4] gives the result of $(A) + (B)$ in (5.11). If we include only the fermionic corrections the T parameter grows from zero to 1.14, while the factor $\bar{\delta}_G$ remains zero. The combination T' then becomes $T' = 1.14 + 0.75 = 1.89$ which gives a too large $\bar{g}_Z^2(0)$ and a too small $\bar{s}^2(m_Z^2)$ as can be read off from (5.12). The fermionic loop gives a dominant contribution to the running of $\bar{g}_Z^2$ below m_Z, and the resulting $\bar{g}_Z^2(m_Z^2) \approx \bar{g}_Z^2(0) + 0.005$ makes the Z boson width unacceptably large. From Table 8, we find that about half of $\chi^2 \sim 500$ in the '+fermion' entry comes from Γ_Z and the rest from the LEP1/SLC asymmetries. In contrast, we find excellent agreement for m_W in the same column. This is mainly because m_W is more sensitive to T rather than to $\bar{\delta}_G$ when α, G_F and m_Z are fixed: $0.42T' - 0.29(T' - T) = 0.42T + 0.13(T' - T)$. Even though there are fortuitous cancellations among the remaining terms, we find no further improvement in the m_W fit by adding extra radiative effects.

It turned out that the 'box-like' corrections to the μ-decay matrix elements amount to almost 80% of the total $\bar{\delta}_G$ value:

$$[\bar{\delta}_G]_{\rm SM} = \bar{\delta}_G^{\rm box} + \bar{\delta}_G^{\rm vertex}\,, \tag{5.13a}$$

$$\bar{\delta}_G^{\rm box} = \frac{\hat{g}_Z^2}{16\pi^2}\Big(\frac{5}{2} - 5\hat{s}^2 + \hat{s}^4\Big)\frac{m_W^2}{m_Z^2 - m_W^2}\log\frac{m_Z^2}{m_W^2}\,, \tag{5.13b}$$

$$\bar{\delta}_G^{\rm vertex} = \frac{\hat{g}^2\hat{c}^2}{16\pi^2}\Big(2 - \frac{m_Z^2 + m_W^2}{m_Z^2 - m_W^2}\log\frac{m_Z^2}{m_W^2}\Big) + \frac{\hat{e}^2}{8\pi^2}\,. \tag{5.13c}$$

Hence by adding the 'box-like' corrections, $\bar{\delta}_G^{\rm box} = 0.00429$, we have $(S', T', U') = (-0.20, 1.30, -0.02)$, and the fit improves significantly. The T' value is still slightly too large, and the '+box' entry still gives too large Γ_Z and too small $\bar{s}^2(m_Z^2)$. This can be seen from the column of '+box', where we give results of $(A) + (B) + (C)$ corrections in (5.11).

These electroweak effects do not affect much the fit of the low energy neutral current experiments because of their larger experimental errors. It is worth noting here that among the electroweak radiative corrections, the 'box-like' ones, especially the WW-box contribution, are most significant in the atomic parity violation experiments. Indeed the fit for $Q_W(C_s)$ improves significantly by adding the 'box-like' corrections.

Up to this stage no contribution from quantum fluctuations with the weak-boson self-couplings are counted. Next the column '+vertex' is considered, where the results of A+B+C+D corrections are listed and where we may hope to see their effects. It turns out that the effects of the remaining 20% correction to $\bar{\delta}_G$ and the effects in part from the vertex corrections in the Z-decay matrix elements considerably reduce the χ^2 in the LEP1/SLC sector of the experiments from about 200 down to 30. The effect of the full $\bar{\delta}_G$ is to change the charge form factor inputs to $(S', T', U') = (-0.20, 1.14, -0.02)$, which reduces $\bar{g}_Z^2(m_Z^2)$ by only 0.1%, increases $\bar{s}^2(m_Z^2)$ by 0.2%. The predicted Γ_Z is reduced by 1% and excellent agreement with the data is found (compare the relevant entries in the '+box' and '+vertex' entries). The major effect of the vertex corrections to Γ_Z is actually coming from the corrections to the Zff vertices in which the corrections from the diagrams with the WWZ vertex, $\overline{\Gamma}_2^f$ in Table 3 of [2], are most significant. The prediction $\bar{s}^2(m_Z^2) = 0.22995$ is still by about 3-σ away from the fit (2.2).

Inclusion of the 'propagator-like' corrections either improves or worsens the fit depending on the Higgs boson mass. The improvement is sizeable only when the Higgs boson mass is not too large, as can be seen from the last column in Table 8.

It is therefore tempting to conclude that the effect of the 'vertex-like' corrections, and hence that of the standard WWV self-interactions is essential for the success of the SM at the quantum correction level. Once the gauge invariance of the weak boson interactions is assumed, quantum fluctuations at very short distances become universal and hence they can be renormalized by precisely measured quantities. Remaining finite parts of the quantum corrections hence measure the effects of the intermediate scale physics which can be sensitive to the symmetry breaking physics. With further improvement of the electroweak data, we will therefore learn more about physics of 100 GeV to 1 TeV that could affect these finite correction terms. The precision electroweak physics may still give us hints of new physics at the energy region which is not yet explored directly by high energy experiments.

6 Impact of future improved measurements

Constraints on various electroweak quantities are expected to be improved in the near future. Their impact on the knowledge of the top and the Higgs masses is discussed in

[4] $m_H = 100$ GeV is chosen to fix the negligible two-loop contributions in the '+fermion' and '+vertex' columns

Table 8. The electroweak data and the SM predictions. The three predictions for Γ_Z, σ_h^0 and R_ℓ are for $\alpha_s = 0.115$, 0.118 and 0.121

	data	no-EW	+fermion	+box	+vertex	+propagator		
m_t (GeV)		——	175	175	175	175	175	175
m_H (GeV)		——	100	——	100	60	300	1000
S		——	-0.067	-0.067	-0.067	-0.283	-0.146	-0.075
T		——	1.136	1.136	1.136	0.910	0.762	0.583
U		——	0.017	0.017	0.017	0.364	0.359	0.358
$\bar{\delta}_G$		——	——	0.00429	0.00549	0.00549	0.00549	0.00549
$1/\bar{\alpha}(m_Z^2)$		128.89	128.90	128.90	128.90	128.75	128.75	128.75
$\bar{s}^2(m_Z^2)$		0.23114	0.22815	0.22955	0.22995	0.23009	0.23094	0.23163
$\bar{g}_Z^2(m_Z^2)$		0.54863	0.55812	0.55569	0.55502	0.55639	0.55592	0.55518
$\bar{\delta}_b(m_Z^2)$		——	——	——	-0.00996	-0.00997	-0.00994	-0.01000
$\bar{s}^2(0)$		0.23866	0.23584	0.23716	0.23753	0.23850	0.23930	0.23995
$\bar{g}_Z^2(0)$		0.54863	0.55321	0.55083	0.55017	0.54926	0.54867	0.54795
$\bar{g}_W^2(0)$		0.42182	0.42713	0.42452	0.42379	0.42449	0.42339	0.42238
Γ_Z(GeV)	2.4946 ± 0.0027	2.4836	2.5346	2.5198	2.4905	2.4963	2.4920	2.4868
		2.4853	2.5364	2.5215	2.4922	2.4980	2.4937	2.4885
		2.4870	2.5381	2.5233	2.4939	2.4997	2.4953	2.4902
σ_h^0(nb)	41.508 ± 0.056	41.507	41.500	41.502	41.489	41.490	41.493	41.496
		41.491	41.484	41.486	41.473	41.474	41.477	41.481
		41.475	41.468	41.470	41.457	41.458	41.461	41.465
R_ℓ	20.778 ± 0.029	20.768	20.817	20.795	20.733	20.731	20.716	20.703
		20.788	20.837	20.815	20.753	20.751	20.736	20.723
		20.808	20.857	20.835	20.773	20.771	20.756	20.743
$A_{\rm FB}^{0,\ell}$	0.0174 ± 0.0010	0.0169	0.0224	0.0198	0.0175	0.0172	0.0157	0.0145
A_τ	0.1401 ± 0.0067	0.1500	0.1732	0.1624	0.1516	0.1505	0.1439	0.1384
A_e	0.1382 ± 0.0076	0.1500	0.1732	0.1624	0.1516	0.1505	0.1439	0.1384
R_b	0.2178 ± 0.0011	0.2182	0.2181	0.2182	0.2156	0.2156	0.2157	0.2157
R_c	0.1715 ± 0.0056	0.1717	0.1719	0.1718	0.1722	0.1722	0.1721	0.1721
$A_{\rm FB}^{0,b}$	0.0979 ± 0.0023	0.1054	0.1219	0.1142	0.1064	0.1056	0.1008	0.0969
$A_{\rm FB}^{0,c}$	0.0735 ± 0.0048	0.0753	0.0883	0.0822	0.0764	0.0758	0.0721	0.0691
$\sin^2\theta_{eff}^{lept}(\langle Q_{\rm FB}\rangle)$	0.2320 ± 0.0010	0.2311	0.2282	0.2296	0.2309	0.2311	0.2319	0.2326
$A_{\rm LR}$	0.1542 ± 0.0037	0.1500	0.1732	0.1624	0.1516	0.1505	0.1438	0.1384
A_b(LR)	0.863 ± 0.049	0.936	0.938	0.937	0.935	0.935	0.934	0.934
A_c(LR)	0.625 ± 0.084	0.669	0.679	0.674	0.670	0.669	0.666	0.664
χ^2	($\alpha_s = 0.115$)	37.1	455.3	181.6	32.3	27.3	24.9	49.5
(d.o.f.=14)	($\alpha_s = 0.118$)	32.4	475.3	194.0	29.0	26.5	21.6	43.4
	($\alpha_s = 0.121$)	29.8	497.2	208.4	27.7	27.6	20.2	39.2
g_L^2	0.2980 ± 0.0044	0.2955	0.3027	0.3049	0.3067	0.3049	0.3036	0.3024
g_R^2	0.0307 ± 0.0047	0.0309	0.0307	0.0307	0.0298	0.0300	0.0301	0.0302
δ_L^2	-0.0589 ± 0.0237	-0.0601	-0.0606	-0.0652	-0.0645	-0.0645	-0.0645	-0.0644
δ_R^2	0.0206 ± 0.0160	0.0186	0.0184	0.0184	0.0179	0.0180	0.0180	0.0181
χ^2		0.4	1.8	3.9	5.5	3.5	2.4	1.5
K (CCFR)	0.5626 ± 0.0060	0.5519	0.5641	0.5685	0.5702	0.5673	0.5653	0.5632
χ^2		3.2	0.1	1.0	1.6	0.6	0.2	0.0
s_{eff}^2	0.233 ± 0.008	0.239	0.236	0.235	0.229	0.230	0.231	0.231
ρ_{eff}	1.007 ± 0.028	1.000	1.008	1.016	1.015	1.013	1.012	1.011
χ^2		0.6	0.1	0.1	0.4	0.2	0.1	0.1
Q_W	-71.04 ± 1.81	-74.73	-74.74	-72.96	-72.92	-73.01	-73.10	-73.14
χ^2		4.2	4.2	1.1	1.1	1.2	1.3	1.3
$2C_{1u} - C_{1d}$	0.938 ± 0.264	0.709	0.725	0.730	0.729	0.724	0.721	0.718
$2C_{2u} - C_{2d}$	-0.659 ± 1.228	0.081	0.099	0.103	0.112	0.106	0.101	0.097
χ^2		1.9	1.2	1.1	1.1	1.2	1.4	1.5
m_W (GeV)	80.356 ± 0.125	79.957	80.459	80.384	80.363	80.429	80.325	80.229
χ^2		10.2	0.7	0.0	0.0	0.3	0.1	1.0
$\chi^2_{\rm tot}$	($\alpha_s = 0.115$)	57.6	463.3	188.8	41.9	34.4	30.3	54.9
(d.o.f.=25)	($\alpha_s = 0.118$)	52.9	483.3	201.3	38.6	33.6	27.0	48.8
	($\alpha_s = 0.121$)	50.3	505.2	215.7	37.3	34.7	25.7	44.7

the following subsections. The last subsection deals with future constraints on the S, T, U parameters.

According to the discussions in the previous section the constraints on the top and the Higgs masses are basically obtained from three quantities, Γ_Z, $\bar{s}^2(m_Z^2)$ from various Z-pole asymmetries, and m_W. After the completion of the LEP1 experiments no further improvement on Γ_Z is expected. Significant improvements in $\bar{s}^2(m_Z^2)$ may be expected from SLC, Tevatron, LHC, and future Linear e^+e^- Colliders (LC). Improved measurements on m_W are also expected from LEP2, Tevatron, LHC, and LC. The top quark mass will be measured accurately at Tevatron, LHC, and LC. The Higgs boson mass can be measured at LEP2, LHC and LC, provided it exists and its mass lies in the accessible energy range of these machines. Finally, a more precise value of $\bar{\alpha}(m_Z^2)$ will be obtained from experiments at Novosibirsk, DAΦNE, B factories at KEK, SLAC and DESY, and possibly at the Beijing τ-charm factory (BTCF).

In order to assess the impact of such future improvements in the electroweak sector, we found the following approximate formulae for the SM predictions useful:

$$\begin{aligned}\Gamma_Z(\,\mathrm{MeV}) \approx\ & 2497.1 + (2.51 - 0.01\,x_H)\,x_t - 2.29\,x_H \\ & -0.65\,x_H^2 + 0.6\,x_\alpha + 1.6\,x_s\,, \qquad (6.1a)\\ \bar{s}^2(m_Z^2) \approx\ & 0.23034 - (0.000335 - 0.000001\,x_H)\,x_t \\ & +0.000518\,x_H + 0.000017\,x_H^2 \\ & -0.00023\,x_\alpha + 0.00001\,x_s\,, \qquad (6.1b)\\ m_W(\,\mathrm{GeV}) \approx\ & 80.400 + (0.0635 - 0.0001\,x_H)\,x_t \\ & -0.0603\,x_H - 0.0062\,x_H^2 \\ & +0.012\,x_\alpha - 0.002\,x_s\,. \qquad (6.1c)\end{aligned}$$

Here $x_t = (m_t - 175\,\mathrm{GeV})/10\,\mathrm{GeV}$, $x_H = \log(m_H/100\,\mathrm{GeV})$, $x_\alpha = (\delta_\alpha - 0.03)/0.09$, and $x_s = (\alpha_s - 0.118)/0.003$. The approximations are valid to 0.2 MeV (6.1a), 0.00002 (6.1b) and 0.003 GeV(6.1c), respectively, in the region $|x_t| < 1$, $|x_\alpha| < 1$, $|x_s| < 1$ and 70 GeV$< m_H <$ 700 GeV. It is instructive to recall that Γ_Z and m_W measure approximately the same combination of m_t, m_H and δ_α: $x_t - 0.9\,x_H + 0.2\,x_\alpha$. The asymmetry parameter $\bar{s}^2(m_Z^2)$ constrains a different combination, which may be approximated as $x_t - 1.5\,x_H + 0.7\,x_\alpha$. Therefore, we need improvements in both m_W and $\bar{s}^2(m_Z^2)$ to reduce the electroweak constraints on m_t and m_H. With the improved direct determination of m_t, each of the above experiments will lead to a significantly better constraint on m_H. The m_H constraint can be strengthened by more precise estimates of $\bar{\alpha}(m_Z^2)$.

6.1 Asymmetries

The different asymmetry measurements from LEP and SLC are in agreement with each other, although showing a large dispersion. The SLD collaboration has contributed the most precise individual determination, namely $\bar{s}^2(m_Z^2) = 0.2294 \pm 0.0005$. The result is dominated by statistics and thus allows for substantial improvement. The average of all other measurements yields $\bar{s}^2(m_Z^2) = 0.2317 \pm 0.0003$. It is instructive to repeat the above SM fit once with A_{LR}^0 alone and then with all other asymmetry data. Figure 15 shows the result in the (m_H, m_t)-plane. Due to the somewhat high value of A_{LR}^0, i.e. low value of $\bar{s}^2(m_Z^2)$, the best-fit value for the Higgs mass turns out to be rather low and most of the allowed region is already excluded by the result of the Higgs searches at LEP1. The complementary fit leads to a best-fit Higgs mass of about 75 GeV, but with a low value for the top quark mass of 152 GeV. The 90% CL allowed region overlaps significantly with the direct information on m_H and m_t. The change in size and orientation of the error ellipses can be understood by considering the SM grid in Fig. 3.

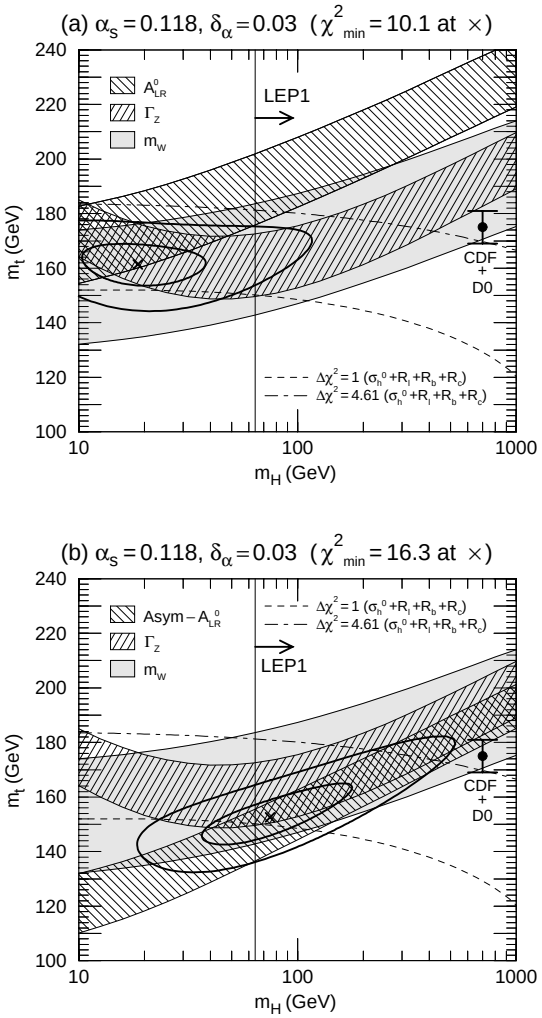

Fig. 15. SM-fit using **a** only the left-right asymmetry by the SLD Collaboration and **b** using all other asymmetry data

Until the start-up of the B-factory the SLD Collaboration hopes to increase their statistics with polarized beams ($P_e \sim 77\%$) to 500k Z-decays, which would allow them to reduce the uncertainty on A_{LR}^0 by a factor of two, without yet hitting the limit set by the systematic error [47]. Such a measurement would determine $\bar{s}^2(m_Z^2)$ to about

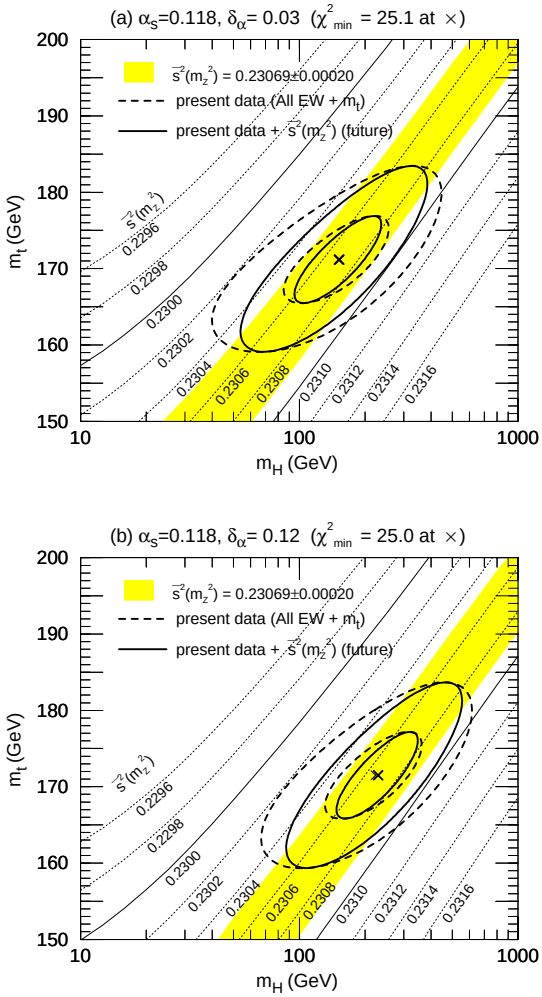

Fig. 16. Impact of future improvement in $\bar{s}^2(m_Z^2)$ in the $(m_H,\, m_t)$ plane, for $\alpha_s = 0.118$ and $\delta_\alpha = 0.03$ **a**, $\delta_\alpha = 0.12$ **b**. An assumed future data $\bar{s}^2(m_Z^2) = 0.23069 \pm 0.00020$ is used to constrain m_t and m_H in addition to the present all electroweak data and the Tevatron m_t data, $m_t = 175 \pm 6\,\mathrm{GeV}$. The *inner* and *outer contours* correspond to $\Delta\chi^2 = 1$ ($\sim$ 39% CL), and $\Delta\chi^2 = 4.61$ ($\sim$ 90% CL), respectively. The minimum of χ^2 is marked by the sign "×". Thin *dotted/solid lines* show the SM predictions for $\bar{s}^2$ when m_t and m_H are given

± 0.00023, i.e. one single experiment is reaching then the same precision as presently all experiments together. With 1M Z-events, the error can be reduced to ± 0.00015. It is clear that a reproduction of the existing mean value with a significantly reduced error would cause a conflict with the other measurements and would put in question the interpretation within the SM.

At hadron colliders the measurement of the lepton forward-backward asymmetries allows to derive also precise values of the weak angle. In the Snowmass'96 report Baur and Demarteau [49] estimate that an uncertainty of 0.00013 can be expected for an integrated luminosity of 30 fb^{-1} at Tevatron [48,50]. The LHC experiments may not improve this further [49] without significantly extending the rapidity coverage of their lepton detector.

The error of $\bar{s}^2(m_Z^2)$ may further be reduced at a future linear e^+e^- collider (LC) by measuring the beam polarization asymmetries on the Z pole, if a significantly improved determination of the electron beam polarization is achieved [51]. It should be emphasised here that the present uncertainty of 0.00023 in theoretical predictions of $\bar{s}^2(m_Z^2)$ due to the uncertainty in $\bar{\alpha}(m_Z^2)$ should not discourage further attempts to improve its measurement, because we anticipate a significant improvement in the $\bar{\alpha}(m_Z^2)$ estimate and also because it leads to a severe constraint on new physics independent of $\bar{\alpha}(m_Z^2)$. Within the SM, precise measurements of $\bar{s}^2(m_Z^2)$ and m_W will reduce the allowed region of m_t and m_H even without improving the $\bar{\alpha}(m_Z^2)$ estimate, because they depend on different combinations of these parameters; see (6.1).

We show in Fig. 16 the impact of future improvement in $\bar{s}^2(m_Z^2)$ in the $(m_H,\, m_t)$ plane, for $\alpha_s = 0.118$ and $\delta_\alpha = 0.03$(a), $\delta_\alpha = 0.12$(b). An assumed future value of

$$\bar{s}^2(m_Z^2) = 0.23069 \pm 0.00020 \tag{6.2}$$

is used to constrain m_t and m_H in addition to the presently available data and the present Tevatron m_t data, $m_t = 175 \pm 6\,\mathrm{GeV}$. The inner and outer contours correspond to $\Delta\chi^2 = 1$ ($\sim$ 39% CL), and $\Delta\chi^2 = 4.61$ ($\sim$ 90% CL), respectively. It is clearly seen that the allowed band in the $(m_H,\, m_t)$ plane is significantly narrowed but the individual error of m_H and m_t is not reduced very much. The sensitivity of the future constraints to $\bar{\alpha}(m_Z^2)$ can be judged by comparing the two figures.

The assumed mean value of 0.23069 is chosen to retain the χ^2_{min} point of the present data. The effect of changing the average and dispersion of the assumed $\bar{s}^2(m_Z^2)$ data can be deduced from the two figures.

6.2 W mass

Improved values on the W mass are expected from CDF, D0 at the Tevatron, from the HERA experiments and from the collaborations at LEP2. It is expected to obtain the W-mass to 31 MeV for a 1 fb^{-1} run at the Tevatron, which may be reduced to 11 MeV for 10 fb^{-1} [49], while at LEP2 in a 500 pb^{-1}-run 35 MeV [52] is expected. In a high luminosity run at HERA a precision of 60 MeV is estimated [53]. Further improved measurements on m_W may be anticipated at a future linear e^+e^- collider [54] or at a $\mu^+\mu^-$ collider [56]. Such measurements will provide a narrow band in the $(m_H\,, m_t)$-plane similar in width and orientation to the present asymmetry band and constitute a crucial piece of information in challenging the validity of the SM.

We show in Fig. 17 the impact of future improvement in W mass measurement in the $(m_H,\, m_t)$ plane, for $\alpha_s = 0.118$ and $\delta_\alpha = 0.03$(a), $\delta_\alpha = 0.12$(b). An assumed future value of

$$m_W(\,\mathrm{GeV}) = 80.350 \pm 0.020 \tag{6.3}$$

is used to constrain m_t and m_H in addition to all the present electroweak data and the present Tevatron value

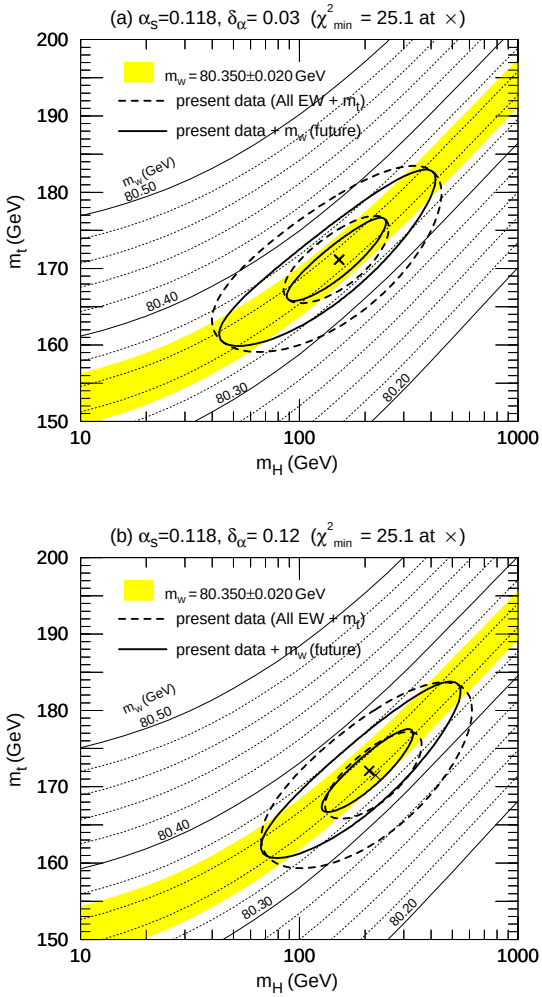

Fig. 17. Impact of future improvement in W mass measurement in the $(m_H,\, m_t)$ plane, for $\alpha_s = 0.118$ and $\delta_\alpha = 0.03$ **a**, $\delta_\alpha = 0.12$ **b**. An assumed future data $m_W = 80.350 \pm 0.020$ is used to constrain m_t and m_H in addition to the present all electroweak data and the Tevatron m_t data, $m_t = 175 \pm 6\,\mathrm{GeV}$. The *inner* and *outer contours* correspond to $\Delta\chi^2 = 1$ ($\sim 39\%$ CL), and $\Delta\chi^2 = 4.61$ ($\sim 90\%$ CL), respectively. The minimum of χ^2 is marked by the sign "×". Thin *dotted/solid lines* show the SM predictions for m_W when m_t and m_H are given

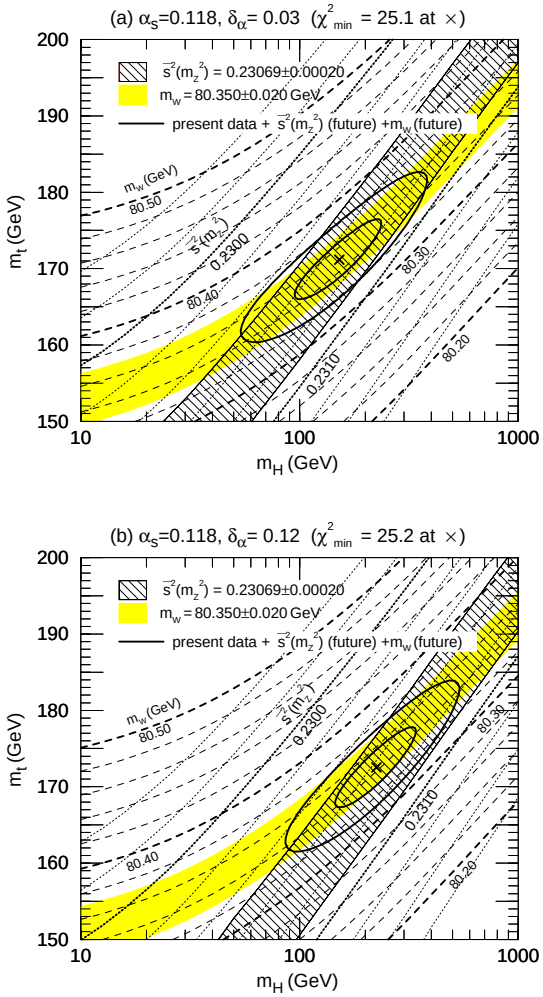

Fig. 18. Impact of future improvement in $\bar{s}^2(m_Z^2)$ and W mass measurements in the $(m_H,\, m_t)$ plane, for $\alpha_s = 0.118$ and $\delta_\alpha = 0.03$ **a**, $\delta_\alpha = 0.12$ **b**. Assumed future data $\bar{s}^2(m_Z^2) = 0.23069 \pm 0.00020$ and $m_W = 80.350 \pm 0.020$ are used to constrain m_t and m_H in addition to the present all electroweak data and the Tevatron m_t data, $m_t = 175 \pm 6\,\mathrm{GeV}$. The *inner* and *outer contours* correspond to $\Delta\chi^2 = 1$ ($\sim 39\%$ CL), and $\Delta\chi^2 = 4.61$ ($\sim 90\%$ CL), respectively. The minimum of χ^2 is marked by the sign "×". Thin *dotted/solid lines* show the SM predictions for m_W when m_t and m_H are given

for the top quark mass, $m_t = 175 \pm 6\,\mathrm{GeV}$. The allowed region in the $(m_H,\, m_t)$ plane shrinks considerably, but the individual errors of m_H and m_t remain essentially unaltered as expected from 6.1. By comparing the two figures, (a) and (b), the sensitivity of the future constraints to $\bar{\alpha}(m_Z^2)$ can be studied.

The assumed mean value of 80.350 GeV is chosen to retain the $\chi^2_{\min}$ point of the present data. The effect of changing the average and dispersion of the assumed m_W data can be deduced from the two figures.

The precise determinations of both $\bar{s}^2(m_Z^2)$ and m_W provide independent constraints on m_t and m_H, as can be clearly seen by overlaying Fig. 16 and Fig. 17. Shown in Fig. 18 is the impact of future improvement in $\bar{s}^2(m_Z^2)$ and W mass measurements in the $(m_H,\, m_t)$ plane, for $\alpha_s = 0.118$ and $\delta_\alpha = 0.03$(a), $\delta_\alpha = 0.12$(b). Assumed future values $\bar{s}^2(m_Z^2) = 0.23069 \pm 0.00020$ and $m_W = 80.350 \pm 0.020$ are shown again by shaded regions. Not only the reduction of the width of the allowed band in the $(m_H,\, m_t)$ plane, but also the individual errors of m_t and m_H are now reduced considerably.

In order to examine the future constraints on $(m_t,\, m_H,\, \delta_\alpha,\, \alpha_s)$ from the electroweak precision measurements, we repeat the four parameter fit with the present electroweak measurements plus the above two additional "data" on $\bar{s}^2(m_Z^2)$ (6.2) and m_W (6.3). We find from the electroweak

data only

$$\left.\begin{aligned} m_t(\,\mathrm{GeV}) &= 161 \pm 5 \\ x_H \quad &= -1.24 \pm 0.95 \\ \alpha_s \quad &= 0.1204 \pm 0.0035 \\ \delta_\alpha \quad &= -0.13 \pm 0.16 \end{aligned}\right\}$$

$$\rho_{\rm corr} = \begin{pmatrix} 1.00 & 0.35 & -0.10 & 0.18 \\ & 1.00 & -0.47 & -0.80 \\ & & 1.00 & 0.42 \\ & & & 1.00 \end{pmatrix}, \tag{6.4a}$$

$$\chi^2_{\rm min}/(\mathrm{d.o.f.}) = 24.6/(23)\,. \tag{6.4b}$$

By comparing with the present constraints (5.1), we find that the error of m_t can be reduced by about a factor of three, that of x_H, i.e. the logarithm of m_H in units of 100 GeV, and δ_α by a factor of two. It may be worth noting that m_t can be predicted to 5 GeV accuracy even without assuming external knowledge on m_H, α_s, and $\bar{\alpha}(m_Z^2)$.

By imposing the present knowledge of m_t, α_s and δ_α, i.e. $m_t = 175 \pm 6\,\mathrm{GeV}$, $\alpha_s = 0.118 \pm 0.003$ and $\delta_\alpha = 0.03 \pm 0.009$, the fit (6.4) becomes

$$\left.\begin{aligned} m_t(\,\mathrm{GeV}) &= 172 \pm 6 \\ x_H \quad &= 0.49 \pm 0.60 \\ \alpha_s \quad &= 0.1190 \pm 0.0022 \\ \delta_\alpha \quad &= 0.04 \pm 0.08 \end{aligned}\right\}$$

$$\rho_{\rm corr} = \begin{pmatrix} 1.00 & 0.84 & 0.13 & -0.26 \\ & 1.00 & 0.13 & -0.63 \\ & & 1.00 & -0.06 \\ & & & 1.00 \end{pmatrix}, \tag{6.5a}$$

$$\chi^2_{\rm min}/(\mathrm{d.o.f.}) = 24.9/(26)\,. \tag{6.5b}$$

This should be compared with the corresponding result in (5.9). It is rather surprising to observe that none of the individual errors of the four fitted parameters reduces significantly from the present errors in (5.9). The mean values stay the same because we chose the mean values of the future $\bar{s}^2(m_Z^2)$ and m_W data at the present minimum of the global χ^2 fit. What did change by adding the above two future "data" are the correlations among the errors, in particular, that between m_t and $\log m_H$ is now very large, 0.84, and the negative correlation between $\log m_H$ and δ_α has also been strengthened. Therefore, we can expect an important improvement on the m_H constraint once m_t and δ_α are measured accurately.

6.3 Top-quark mass

It is tantalizing that the present top mass value from Tevatron (5.7) lies just on the boundary of the region allowed by the electroweak data.

The long-range program (TeV33 [48,50]) at the Tevatron envisages an ultimate precision of the top mass of about 2 GeV based on an anticipated yearly integrated luminosity of 10 fb^{-1}. In the future, the error can be reduced further to 200 MeV at an e^+e^- LC [55] and possibly down to 70 MeV at a muon collider [56] with precise beam energy resolution. Figure 13 shows us that once the top quark mass is precisely determined, the major remaining uncertainty in electroweak fits is due to δ_α, the magnitude of the QED running coupling constant at the m_Z scale.

Next we examine the effect of a future measurement $m_t = 175 \pm 2$ GeV on the four parameter fit (6.5):

$$\left.\begin{aligned} m_t(\,\mathrm{GeV}) &= 175 \pm 2 \\ x_H \quad &= 0.75 \pm 0.35 \\ \alpha_s \quad &= 0.1192 \pm 0.0021 \\ \delta_\alpha \quad &= 0.05 \pm 0.08 \end{aligned}\right\}$$

$$\rho_{\rm corr} = \begin{pmatrix} 1.00 & 0.48 & 0.05 & -0.09 \\ & 1.00 & 0.07 & -0.73 \\ & & 1.00 & -0.03 \\ & & & 1.00 \end{pmatrix}, \tag{6.6a}$$

$$\chi^2_{\rm min}/(\mathrm{d.o.f.}) = 25.2/(26)\,. \tag{6.6b}$$

The error of the logarithm of m_H has been reduced from ± 0.60 (6.5) to ± 0.35, which is substantial, but not satisfactory. We find that this error cannot be reduced significantly by further reducing the error of m_t down to 1 GeV. This may be inferred from the reduced correlation between m_t and $\log m_H$ in (6.6). The strongest correlation among the four errors now appears between $\log m_H$ and δ_α. It is clear that further progress about m_H in the SM, and also about physics beyond the SM from its quantum effects, will critically depend on an improved determination of $\bar{\alpha}(m_Z^2)$.

As a final example, we present the four parameter fit result with one further constraint, $\delta_\alpha = 0.03 \pm 0.03$, where the error is assumed to be 1/3 of the conservative estimate [18], or 1/2 of the other two estimates [16,17]. We find

$$\left.\begin{aligned} m_t(\,\mathrm{GeV}) &= 175 \pm 2 \\ x_H \quad &= 0.69 \pm 0.26 \\ \alpha_s \quad &= 0.1192 \pm 0.0021 \\ \delta_\alpha \quad &= 0.03 \pm 0.03 \end{aligned}\right\}$$

$$\rho_{\rm corr} = \begin{pmatrix} 1.00 & 0.58 & 0.05 & -0.04 \\ & 1.00 & 0.07 & -0.38 \\ & & 1.00 & -0.01 \\ & & & 1.00 \end{pmatrix}, \tag{6.7a}$$

$$\chi^2_{\rm min}/(\mathrm{d.o.f.}) = 25.3/(26)\,. \tag{6.7b}$$

The error in $\log m_H$ is now reduced to about ± 0.25.

To conclude, we examine the constraint on m_H from ultimate electroweak measurements by making use of the expressions (6.1). With the top-quark mass determination of order 100 MeV at a LC or at a muon collider, its error can be safely neglected in (6.1). Once the α_s value is measured to the 1% level [57], the LEP1 constraint from Γ_Z becomes more effective through (6.1a). Nevertheless we find that m_H will be constrained essentially by the future

measurements of $\bar{s}^2(m_Z^2)$ and m_W within the SM:

$$\Delta[\,x_H - 0.44\,x_\alpha\,] = \pm\frac{\Delta\bar{s}^2(m_Z^2)}{0.0005}\,, \tag{6.8}$$

$$\Delta[\,x_H - 0.20\,x_\alpha\,] = \pm\frac{\Delta m_W(\,\mathrm{GeV})}{0.06}\,. \tag{6.9}$$

Combining the above two constraints (6.8) and (6.9) gives

$$\Delta[\,x_H - A\,x_\alpha\,] = \pm\sigma\,, \tag{6.10a}$$

$$\Delta x_\alpha = \pm\sigma_\alpha\,, \tag{6.10b}$$

with

$$\frac{1}{\sigma^2} \approx (\frac{0.0005}{\Delta\bar{s}^2(m_Z^2)})^2 + (\frac{0.06}{\Delta m_W})^2\,, \tag{6.11a}$$

$$\frac{A}{\sigma^2} \approx 0.44\,(\frac{0.0005}{\Delta\bar{s}^2(m_Z^2)})^2 + 0.20\,(\frac{0.06}{\Delta m_W})^2\,, \tag{6.11b}$$

$$\frac{1}{\sigma_\alpha^2} \approx 0.19\,(\frac{0.0005}{\Delta\bar{s}^2(m_Z^2)})^2 + 0.04\,(\frac{0.06}{\Delta m_W})^2 - \frac{A^2}{\sigma^2} + \frac{1}{(\Delta x_\alpha^{(\mathrm{ext})})^2}\,, \tag{6.11c}$$

where $\Delta x_\alpha^{(\mathrm{ext})} = \Delta[1/\bar{\alpha}(m_Z^2)]/0.09$ is the external constraint on $\bar{\alpha}(m_Z^2)$. For instance, with $\Delta\bar{s}^2(m_Z^2) = 0.00010$, $\Delta m_W(\,\mathrm{GeV}) = 0.010$, and $\Delta x_\alpha^{(\mathrm{ext})} = 0.30$, we find $\Delta[\,x_H - 0.30\,x_\alpha\,] = \pm 0.13$ with $\Delta x_\alpha = \pm 0.29$. Hence with the above ultimate assumptions, the error of the SM prediction to $\log m_H$ reduces to ± 0.15. On the other hand, once the Higgs boson is found, its mass may be measured so accurately that its error can be neglected in the electroweak radiative effects. The electroweak data (6.8) and (6.9) then constrain δ_α to ± 0.036, or about 40% its present error [18]. Evidence for new physics may then be looked for by comparing the direct and indirect measurements of $\bar{\alpha}(m_Z^2)$.

6.4 Future constraints on S, T, U

The impact on S, T, U of the future measurements of $\bar{s}^2(m_Z^2)$ (6.2) and m_W (6.3) is discussed briefly in this subsection. The analysis of Sect. 4.4 can be repeated straightforwardly.

It is again worth noting that only the following combinations of these parameters and δ_α, $\bar{\delta}_G$ and α_s can be constrained by the three most accurately measurable quantities:

$$\Gamma_Z(\,\mathrm{MeV}) \approx 2473.0 - 9.5\,S' + 25.0\,T' + 1.7\,x_s' - 3.4\,\log[\,1 + (\frac{26\,\mathrm{GeV}}{m_H})^2\,]\,, \tag{6.12a}$$

$$\bar{s}^2(m_Z^2) \approx 0.2334 + 0.0036\,S' - 0.0024\,T' \tag{6.12b}$$

$$m_W(\,\mathrm{GeV}) \approx 79.840 - 0.291\,S' + 0.417\,T' + 0.332\,U''\,. \tag{6.12c}$$

Here $x_s' = (\alpha_s' - 0.118)/0.003 = [\alpha_s - 0.118 + 1.54\,(\bar{\delta}_b + 0.00995)]/0.003$, and

$$S' = S - 0.72\,\delta_\alpha\,, \tag{6.13a}$$

$$T' = T + (0.0055 - \bar{\delta}_G)/\alpha\,, \tag{6.13b}$$

$$U'' = U' - 0.87\,(T' - T) = U - 0.22\,\delta_\alpha + 0.87\,(0.0055 - \bar{\delta}_G)/\alpha\,. \tag{6.13c}$$

A linear combination of S' and T' will be better constrained by future improvements in $\bar{s}^2(m_Z^2)$. Individual constraints will still be obtained from the LEP1 Γ_Z value, and hence they won't be improved significantly unless one can predict accurately the α_s' value including the Zb_Lb_L vertex factor. The improved measurement on m_W determines the combination U''. Therefore, we need to know $\bar{\delta}_b$, $\bar{\delta}_G$ and δ_α accurately in order to constrain non-SM contributions to the S, T, U parameters.

As an example consider the result of the three parameter fit with the new $\bar{s}^2(m_Z^2)$ and m_W measurements of (6.2) and (6.3), respectively:

$$\left.\begin{aligned} S' &= -0.32 - 0.061\,\tfrac{\alpha_s' - 0.1075}{0.0037} \pm 0.11 \\ T' &= 0.61 - 0.096\,\tfrac{\alpha_s' - 0.1075}{0.0037} \pm 0.14 \\ U'' &= 0.47 + 0.065\,\tfrac{\alpha_s' - 0.1075}{0.0037} \pm 0.11 \end{aligned}\right\}$$

$$\rho_{\mathrm{corr}} = \begin{pmatrix} 1 & 0.92 & -0.60 \\ & 1 & -0.79 \\ & & 1 \end{pmatrix}, \tag{6.14a}$$

$$\chi^2_{\mathrm{min}} = 20.4 + \left(\frac{\alpha_s' - 0.1075}{0.0037}\right)^2 + \left(\frac{\bar{\delta}_b + 0.0051}{0.0028}\right)^2, \quad (\mathrm{d.o.f.} = 23)\,. \tag{6.14b}$$

As compared to the present result (4.24), we find substantial reductions in the error of U'' but not in those of S' and T' individually. On the other hand, all correlations are stronger compared to those of (4.24). The most stringent constraint among the S, T, U parameters now reads

$$T' - 0.96S' + 0.45U'' = 1.13 \pm 0.036. \tag{6.15}$$

When compared with the corresponding constraint (4.25) of the existing electroweak data, the allowed range of T' for given S' and U' can be reduced by a factor of two.

7 Conclusions

We have carried out a comprehensive analysis of the latest electroweak data. The analysis updates our previous work (see [2]). The total width Γ_Z, the hadronic width Γ_h^0 and the leptonic width Γ_ℓ agree well with the SM predictions at the level of a few 10^{-3}. The new measurement of R_c is in agreement with the SM, and also the new measurement of R_b, albeit within about two standard deviations. The asymmetry data determine the effective weak mixing

parameter $\sin^2\theta_W$ to an accuracy of 0.1% level, see (2.2). Their average value agrees well with the SM, while their dispersion is larger than statistically expected. It is, however, fair to conclude that the progress both in precision and agreement of data with SM expectation is impressive.

The (S, T) fit agrees well with the SM, whereas the simple QCD-like Techni-Color (TC) model is ruled out at the 99% CL. The fitted U parameter also agrees with the SM prediction. The fact that all the S, T, U parameters agree well with the SM prediction for the top quark mass as observed at the Tevatron and the Higgs boson mass below a few hundred GeV implies that any dynamical model of the electroweak symmetry breaking without a light Higgs boson should not only give a negative $S_{\rm new}$, but also a $T_{\rm new}$-value which is constrained severely by the data for the given $S_{\rm new}$ and $U_{\rm new}$; see (4.25). The above conclusion remains valid even if the model contributes a sizeable amount to the Zb_Lb_L vertex, since the strong correlation between $S_{\rm new}$ and $T_{\rm new}$ comes from the accurate measurement of the effective weak mixing angle, $\bar{s}^2(m_Z^2)$, which is independent of R_b or the assumed α_s value. For the U parameter, $|U_{\rm new}|\lesssim 0.4$ should be satisfied. The uncertainty in the running QED coupling constant at the m_Z scale, $\bar{\alpha}(m_Z^2)$, is shown as *the* serious limiting factor for future improvements in the determination of the S parameter.

The global fit in the minimal SM in terms of (m_t, m_H) yields values for the top mass, $m_t = 153 \pm 10\,\text{GeV}$ (5.2a), or $m_t = 158 \pm 12\,\text{GeV}$ (5.4a) if we drop the present R_b constraint, which agrees with the direct measurements from the Tevatron, $m_t = 175 \pm 6\,\text{GeV}$ [8]. The corresponding allowed range in m_H is $m_H = 50^{+50}_{-30}\,\text{GeV}$ (5.2a) and $m_H = 60^{+100}_{-40}\,\text{GeV}$ (5.4a) respectively. Once m_t is accurately measured the present electroweak data will impose stringent limits on the Higgs-boson mass which are not affected by the R_b data (see Table 7 in Sect. 5.2). For instance the present electroweak data favor a light Higgs boson if $m_t \lesssim 170\,\text{GeV}$ while a heavier Higgs boson is favored if $m_t \gtrsim 180\,\text{GeV}$: the 95% CL upper and lower mass bounds, $m_H < 360\,\text{GeV}$ for $m_t = 170\,\text{GeV}$ and $m_H > 130\,\text{GeV}$ for $m_t = 180\,\text{GeV}$ are obtained by using $\alpha_s = 0.118 \pm 0.003$ [28] and $\delta_\alpha = 0.03 \pm 0.09$ [18]. In order to further improve the constraint on m_H not only precise measurement on m_t are required, but also improved measurements on $\Delta\alpha_{\rm had}(m_Z^2)$ and α_s.

For the agreement of the SM predictions with precision experiments it is indispensable to include radiative effects due to 'vertex-like' corrections which may be regarded as indirect evidence for the universal weak-boson self-couplings. Their direct investigation will soon be carried out at LEP 2.

Finally, we studied prospects of future improvements in the electroweak precision experiments. Major improvements are expected from further running and detector upgrades in the determination of the mixing parameter $\bar{s}^2(m_Z^2)$ at SLC, Tevatron, and at a future linear e^+e^- collider (LC); m_W will be measured more accurately at LEP2, Tevatron upgrades, LHC, LC and, perhaps, at a muon collider. The error in the top-quark mass may be reduced to 2 GeV at Tevatron, 200 MeV at LC, and even further down at a muon collider. These measurements will constrain physics beyond the SM very stringently, say in the $(S_{\rm new}, T_{\rm new}, U_{\rm new})$ parameter space, where not only $T_{\rm new}$ but also $U_{\rm new}$ will be constrained severely as function of $S_{\rm new}$, whose constraint can be improved with a better $\alpha(m_Z^2)$ knowledge. Within the SM, the constraint on the Higgs boson mass will not improve significantly beyond ± 0.35 for $\log m_H$, unless a substantial improvement in the $\alpha(m_Z^2)$ estimate is achieved also.

Acknowledgements. We would like to thank S. Aoki, U. Baur, B.K. Bullock, D. Charlton, M. Drees, S. Eidelman, S. Erredi, G.L. Fogli, W. Hollik, R. Jones, J. Kanzaki, J.H. Kühn, C. Mariotti, A.D. Martin, K. McFarland, T. Mori, M. Morii, D.R.O. Morrison, B. Pietrzyk, P.B. Renton, P. Rowsen, M.H. Shaevitz, D. Schaile, M. Swartz, R. Szalapski, T. Takeuchi, P. Vogel, P. Wells and D. Zeppenfeld for discussions.

References

1. The LEP Collaborations ALEPH, DELPHI, L3, OPAL, the LEP Electroweak Working Group and the SLD Heavy Flavour Group, preprint CERN-PPE/96-183 (December 1996)
2. K. Hagiwara, D. Haidt, C.S. Kim and S. Matsumoto, Z. Phys. **C64**, 559 (1994); **C68** (1995) 352(E)
3. S. Matsumoto, Mod. Phys. Lett. **A10**, 2553 (1995)
4. The LEP Collaborations ALEPH, DELPHI, L3, OPAL and the LEP Electroweak Working Group, preprint CERN-PPE/95-172 (1995)
5. M.E. Peskin and T. Takeuchi, Phys. Rev. Lett. **65**, 964 (1990); Phys. Rev. **D46**, 381 (1992)
6. M. Rijssenbeek, talk at ICHEP96, Warsaw, 25-31 July 1996, Fermilab-Conf-96-365-E, to appear in the proceedings
7. K. McFarland, talk at the XV Workshop on Weak Interactions and Neutrinos, Talloires, France, 4–8 Sep 1995
8. CDF Collaboration, J. Lys, talk at ICHEP96, Warsaw, 25-31 July 1996, Fermilab-Conf-96-409-E, to appear in the proceedings;
   D0 Collaboration, S. Protopopescu, talk at ICHEP96, Warwaw, 25-31 July 1996, to appear in the proceedings;
   P. Tipton, talk at ICHEP96, Warsaw, 25-31 July 1996, to appear in the proceedings
9. K. Hagiwara, Proceedings of 17th International Symposium on Lepton-Photon Interactions(LP95) (Beijing, P.R. China, 10-15 August 1995), p. 63
10. J.M. Cornwall and J. Papavassiliou, Phys. Rev. **D40**, 3474 (1989);
    J. Papavassiliou and K. Phillippides, ibid. **48** (1993) 4225; ibid. **51** (1995) 6364;
    J. Papavassiliou, ibid. **50** (1994) 5998
11. G. Degrassi and A. Sirlin, Nucl. Phys. **B383**, 73 (1992); Phys. Rev. **D46**, 3104 (1992); G. Degrassi, B. Kniehl and A. Sirlin, ibid. **48** (1993) R3963
12. D.C. Kennedy and B.W. Lynn, Nucl. Phys. **B322**, 1 (1989)
13. K. Hagiwara, S. Matsumoto and R. Szalapski, Phys. Lett. **B357**, 411 (1995); K. Hagiwara, T. Hatsukano,

R. Ishihara and R. Szalapski, preprint KEK-TH-497, hep-ph/9612268, to appear in Nucl. Phys. B
14. J. Papavassiliou, E. de Rafael and N.J Watson, Preprint CPT-96-P-3408, hep-ph/9612237
15. A. Sirlin, Phys. Rev. **D22**, 971 (1980)
16. A.D. Martin and D. Zeppenfeld, Phys. Lett. **B345**, 558 (1995)
17. M.L. Swartz, Phys. Rev. **D53**, 5268 (1995)
18. S. Eidelman and F. Jegerlehner, Z. Phys. **C67**, 602 (1995)
19. H. Burkhardt and B. Pietrzyk, Phys. Lett. **B356**, 398 (1995)
20. B.A. Kniehl, Nucl. Phys. **B347**, 86 (1990)
21. H. Burkhardt, F. Jegerlehner, G. Penso and C. Verzegnassi, Z. Phys. **C43**, 497 (1989)
22. F. Jegerlehner, in Testing the Standard Model, eds. M. Cvetič and P. Langacker (World Scientific, 1991)
23. F. Jegerlehner, cited by B.A. Kniehl in Proc. Europhysics Marseille 1993, p. 639
24. K.G. Chetyrkin, J.H. Kühn and M. Steinhauser, Phys. Lett. **B351**, 331 (1995);
L. Avdeev, J. Fleischer, S. Mikhailov and O. Tarasov, Phys. Lett. **B336**, 560 (1994); Erratum ibid. **349** 597 (1995)
25. K.G. Chetyrkin, J.H. Kühn and M. Steinhauser, Phys. Rev. Lett. **75**, 3394 (1995)
26. A. Czarnecki and J.H. Kühn, Phys. Rev. Lett. **77**, 3955 (1996)
27. P.B. Renton, Proceedings of 17th International Symposium on Lepton Photon Interactions (LP95) (Beijing, P.R. China, 10–15 August 1995), p35
28. Particle Data Group, R.M. Barnett et al., Phys. Rev. **D54**, 1 (1996)
29. The OPAL Collaboration, G. Alexander et al., Z. Phys. **C72**, 1 (1996)
30. The OPAL Collaboration, K. Ackerstaff et al., preprint CERN-PPE/96-167 (Nov 1996)
31. The ALEPH Collaboration, talk by J.Steinberger in CERN Seminar, : 8 Oct 1996;
The ALEPH Collaboration, R. Barate et al., Preprint CERN-PPE/97-017;
The ALEPH Collaboration, R. Barate et al., Preprint CERN-PPE/97-018
32. G.L. Fogli and D. Haidt, Z. Phys. **C40**, 379 (1988)
33. P. Langacker, in Precision Tests of the Standard Electroweak Model, ed. by P. Langacker (World Scientific, 1994)
34. T. Appelquist and J. Terning, Phys. Lett. **B315**, 139 (1993); Phys. Rev. **D50**, 2116 (1994)
35. J. Ellis, G.L. Fogli and E. Lisi, Phys. Lett. **B343**, 282 (1995)
36. G. Altarelli, talk at the NATO Advanced Study Institute on Techniques and Concepts of High Energy Physics, St. Croix, 10–23 July 1996, hep-ph/9611239
37. P. Langacker and J. Erler, presented at the Ringberg Workshop on the Higgs Puzzle, December 1996, hep-ph/9703428
38. J.L. Rosner, hep-ph/9704331, submitted to Comments on Nuclear and Particle Physics
39. J. Ellis, G.L. Fogli and E. Lisi, Phys. Lett. **B389**, 321 (1996)
40. W. de Boer, A. Dabelstein, W. Hollik, W. Mösle and U. Schwickerath, hep-ph/9609209 v4 (Nov, 1996)
41. V.A. Novikov, L.B. Okun and M.I. Vysotsky, Mod. Phys. Lett. **A8**, 2529 (1993); Erratum **A8** 3301 (1993)
42. Y. Okada, M. Yamaguchi, T. Yanagida, Prog. Theor. Phys. **85**, 1 (1991); Phys. Lett. **B262**, 54 (1991); H. Haber, R. Hempfling, Phys. Rev. Lett. **66**, 1815 (1991); Phys. Lett. **B262**, 54 (1991); J. Ellis, G. Ridorfi, F. Zwirner, Phys. Lett. **B257**, 83 (1991); Phys. Lett. **B262**, 477 (1991)
43. J.D. Bjorken, Phys. Rev. **D19**, 335 (1978); P.D. Hung and J.J. Sakurai, Nucl. Phys. **B143**, 81 (1978)
44. P. Gambio and A. Sirlin, Phys. Rev. Lett. **73**, 621 (1994)
45. K. Hagiwara, Proceedings of the International Symposium on Vector Boson Self-Interactions, eds. U. Baur, S. Errede and T. Müller (Los Angeles, 1995, AIP Press), p. 185
46. V.A. Novikov, L.B. Okun, A.N. Rozanov and M.I. Vysotsky, Mod. Phys. Lett. **A9**, 2641 (1994); Z. Hioki, Phys. Lett. **B340**, 181 (1994)
47. P. Rowson, private communication
48. D. Amidei et al., Preprint CDF/DOC/TOP/PUBLIC/3265 (Aug 1995)
49. U. Baur and M. Demarteau, Precision electroweak physics at future collider experiments, hep-ph/9611334 v2, to be published in Proceedings of the 1996 DPF/DPB Summer Study on New Directions for High-Energy Physics (Snowmass 96)
50. D. Amidei and R. Brock, Future electroweak physics at the Fermilab Tevatron: Report of the TeV2000 Study Group, Fermilab-Pub-96/082 (April 1996)
51. T. Omori, Proceedings of the 2'nd Workshop on JLC , ed. by S. Kawabata, KEK Proceedings 91-10, p. 315
52. A. Ballestrero et al., Proceedings of the Workshop on Physics at LEP2, G. Altarelli, T. Sjöstrand and F. Zwirner (eds.), CERN Yellow Report CERN 96-01 (1996), Vol.1, p. 141
53. R.J. Cashmore et al., MPI/PTh/96-105 and Proceedings of the Workshop on future Physics at HERA 1996
54. A. Miyamoto, Physics and Experiments with Linear e^+e^- Colliders, edited by F.A. Harris et al. (World Scientific, 1993), p. 141
55. L.H. Orr, Physics and Experiments with Linear e^+e^- Colliders, eds. A.Miyamoto et al. (World Scientific, 1996), p. 129
56. V. Barger, M.S. Berger, J.F. Gunion and T. Han, "Precision W-boson and top-quark mass determination at a muon collider", hep-ph/9702334
57. P.N. Burrows et al., "Prospects for the precision measurement of α_s", hep-ex/9612012, to be published in Proceedings of the 1996 DPF/DPB Summer Study on New Directions for High-Energy Physics (Snowmass 96)